National Institute of
Environmental Health Sciences

NIEHS Report on the In Vivo Repeat Dose Biological Potency Study of Perfluorohexanesulfonamide (CASRN 41997-13-1) in Sprague Dawley (Hsd:Sprague Dawley® SD®) Rats (Gavage Studies)

NIEHS 10

March 2023

NIEHS Report on the In Vivo Repeat Dose Biological Potency Study of Perfluorohexanesulfonamide (CASRN 41997-13-1) in Sprague Dawley (Hsd:Sprague Dawley® SD®) Rats (Gavage Studies)

NIEHS Report 10

March 2023

National Institute of Environmental Health Sciences
Public Health Service
U.S. Department of Health and Human Services
ISSN: 2768-5632

Research Triangle Park, North Carolina, USA

Foreword

The National Institute of Environmental Health Sciences (NIEHS) is one of 27 institutes and centers of the National Institutes of Health, which is part of the U.S. Department of Health and Human Services. The NIEHS mission is to discover how the environment affects people in order to promote healthier lives. NIEHS works to accomplish its mission by conducting and funding research on human health effects of environmental exposures; developing the next generation of environmental health scientists; and providing critical research, knowledge, and information to citizens and policymakers who are working to prevent hazardous exposures and reduce the risk of disease and disorders connected to the environment. NIEHS is a foundational leader in environmental health sciences and committed to ensuring that its research is directed toward a healthier environment and healthier lives for all people.

The NIEHS Report series began in 2022. The environmental health sciences research described in this series is conducted primarily by the Division of Translational Toxicology (DTT) at NIEHS. NIEHS/DTT scientists conduct innovative toxicology research that aligns with real-world public health needs and translates scientific evidence into knowledge that can inform individual and public health decision-making.

NIEHS reports are available free of charge on the NIEHS/DTT website and cataloged in PubMed, a free resource developed and maintained by the National Library of Medicine (part of the National Institutes of Health).

Table of Contents

Tables

About This Report

Authors

Scott S. Auerbach[1], Jeff D. Ballin[2], James C. Blake[3], Donna B. Browning[3], Bradley J. Collins[1], Michelle C. Cora[1], Reshan A. Fernando[3], Jennifer M. Fostel[1], Ying F. Liu [4], Jeanne Luh[5], Nicholas J. Machesky[2], Lisa M. Prince[5], Georgia K. Roberts[1], Kelly A. Shipkowski[1], Melanie A.R. Silinski[3], Anthony J. Skowronek[2], Barney R. Sparrow[2], Heather Toy [6], Suramya Waidyanatha[1], AtLee T.D. Watson[1]

[1]Division of Translational Toxicology, National Institute of Environmental Health Sciences, Research Triangle Park, North Carolina, USA

[2]Battelle, Columbus, Ohio, USA

[3]RTI International, Research Triangle Park, North Carolina, USA

[4]ASRC Federal, Research Triangle Park, North Carolina, USA

[5]ICF, Reston, Virginia, USA

[6]AmplifyBio, West Jefferson, Ohio, USA

Division of Translational Toxicology, National Institute of Environmental Health Sciences, Research Triangle Park, North Carolina, USA
Evaluated and interpreted the results and reported findings; developed reporting framework
Scott S. Auerbach, Ph.D., Study Scientist
Michelle C. Cora, D.V.M.
Georgia K. Roberts, Ph.D.
Kelly A. Shipkowski, Ph.D.
AtLee T.D. Watson, Ph.D.

Coordinated data integration
Jennifer M. Fostel, Ph.D.

Analyzed and interpreted analytical chemistry data
Bradley J. Collins, M.S.P.H.
Suramya Waidyanatha, Ph.D.

Battelle, Columbus, Ohio, USA
Provided contract oversight
Barney R. Sparrow, Ph.D.

Conducted in-life studies
Anthony J. Skowronek, D.V.M., Ph.D.

Performed RNA isolation
Nicholas J. Machesky, Ph.D.

Conducted thyroid biomarker analysis
Jeff D. Ballin, Ph.D.

AmplifyBio, West Jefferson, Ohio, USA
Compiled results
Heather Toy, B.S., Study Director

RTI International, Research Triangle Park, North Carolina, USA
Conducted prestart chemistry activities, dose formulations, and biological sample chemistry analyses of total thyroid hormone levels
Reshan A. Fernando, Ph.D., Principal Investigator
James C. Blake, B.A., Deputy Principal Investigator
Donna B. Browning, B.S.
Melanie A.R. Silinski, Ph.D.

ICF, Reston, Virginia, USA
Contributed to technical writing and data integration and ensured report quality
Jeanne Luh, Ph.D.
Lisa M. Prince, Ph.D.

ASRC Federal, Research Triangle Park, North Carolina, USA
Developed data tables and supplemental materials
Ying F. Liu, Ph.D.

Contributors

Division of Translational Toxicology, National Institute of Environmental Health Sciences, Research Triangle Park, North Carolina, USA
Critically reviewed report and results
John R. Bucher, Ph.D.
Fred M. Parham, Ph.D.
Nigel J. Walker, Ph.D.

Contributed to development and review of reporting framework
Michael J. DeVito, Ph.D.
William M. Gwinn, Ph.D.
Alison H. Harrill, Ph.D.
Scott A. Masten, Ph.D.
Matthew D. Stout, Ph.D.
Greg S. Travlos, D.V.M.
Mary S. Wolfe, Ph.D.

Developed and updated BMDS software package
Andrew J. Shapiro, M.S.P.H.

ASRC Federal, Research Triangle Park, North Carolina, USA
Developed data tables and supplemental materials
Julie Berke, B.S.
Shihan He, Ph.D.
Christina Myers, M.S.

CSS Corporation, Research Triangle Park, North Carolina, USA
Prepared quality assessment audits
Steven Brecher, Ph.D., Principal Investigator
Sudha Iyer, B.S.
Varghese S. Tharakan, D.V.M

Sciome LLC, Research Triangle Park, North Carolina, USA
Provided bioinformatics analysis
Michele R. Balik-Meisner, Ph.D.
Dhiral P. Phadke, M.S.
Ruchir R. Shah, Ph.D.

ICF, Reston, Virginia, USA
Provided contract oversight
David F. Burch, M.E.M., Principal Investigator
Cary E. Haver, M.P.H.
Jessica A. Wignall, M.S.P.H.

Prepared and edited report
Lauren M. Browning, M.S.
Katherine S. Duke, Ph.D.
Tara Hamilton, M.S.
Pamela A. Hartman, M.E.M.
Samantha J. Snow, Ph.D.
Jonathan R. Thompson, B.S.
Nkoli Ukpabi, M.S.

Peer Review

This report was modeled after the *NTP Research Report on In Vivo Repeat Dose Biological Potency Study of Triphenyl Phosphate (CAS No. 115-86-6) in Male Sprague Dawley (Hsd:Sprague Dawley® SD®) Rats (Gavage Studies)* (https://doi.org/10.22427/NTP-RR-8), which was reviewed internally at the National Institute of Environmental Health Sciences and peer reviewed by external experts. Importantly, these reports employ mathematical model-based approaches to identify and report potency of dose-responsive effects and do not attempt more subjective interpretation (i.e., make calls or reach conclusions on hazard). The peer reviewers of the initial 5-day research report determined that the study design, analysis methods, and results presentation were appropriate. The study design, analysis methods, and results presentation employed for this study are identical to those previously reviewed, approved, and reported; therefore, following internal review, the *NIEHS Report on the In Vivo Repeat Dose Biological Potency Study of Perfluorohexanesulfonamide (CASRN 41997-13-1) in Sprague Dawley (Hsd:Sprague Dawley® SD®) Rats (Gavage Studies)* was not subjected to further external peer review.

Publication Details

Publisher: National Institute of Environmental Health Sciences

Publishing Location: Research Triangle Park, NC

ISSN: 2768-5632

DOI: https://doi.org/10.22427/NIEHS-10

Report Series: NIEHS Report Series

Report Series Number: 10

Official citation: Auerbach SS, Ballin JD, Blake JC, Browning DB, Collins BJ, Cora MC, Fernando RA, Fostel JM, Liu YF, Luh J, Machesky NJ, Prince LM, Roberts GK, Shipkowski KA, Silinski MAR, Skowronek AJ, Sparrow BR, Toy H, Waidyanatha S, Watson ATD. 2023. NIEHS report on the in vivo repeat dose biological potency study of perfluorohexanesulfonamide (CASRN 41997-13-1) in Sprague Dawley (Hsd:Sprague Dawley® SD®) rats (gavage studies). Research Triangle Park, NC: National Institute of Environmental Health Sciences. NIEHS Report 10.

Acknowledgments

This work was supported by the Intramural Research Program (ES103316, ES103318, ES103319, and ES102505) at the National Institute of Environmental Health Sciences (NIEHS), National Institutes of Health and performed for NIEHS under contracts HHSN273201800006C, HHSN273201700005C, HHSN273201700001C, GS00Q14OADU417 (Order No. HHSN273201600015U), HHSN273201500006C, HHSN273201400022C, HHSN273201300004C, and HHSN316201200054W.

Abstract

Background: Perfluorohexanesulfonamide (PFHxSAm) is a member of the per- and polyfluoroalkyl class of compounds to which humans are widely exposed. Toxicological information on this class of chemicals is sparse. A short-term, in vivo transcriptomic study was used to assess the biological potency of PFHxSAm.

Methods: A short-term in vivo biological potency study on PFHxSAm in adult male and female Sprague Dawley (Hsd:Sprague Dawley® SD®) rats was conducted. PFHxSAm was formulated in acetone:corn oil (1:99) and administered once daily for 5 consecutive days by gavage (study days 0–4). PFHxSAm was administered at 10 doses (0, 0.15, 0.5, 1.4, 4, 12, 37, 111, 333, and 1,000 mg/kg body weight [mg/kg]). Blood was collected from animals dedicated for internal dose assessment in the 4 and 37 mg/kg groups. On study day 5, the day after the final dose was administered, animals were euthanized, standard toxicological measures were assessed, and the liver and kidney were assayed in gene expression studies using the TempO-Seq assay. Modeling was conducted to identify the benchmark doses (BMDs) associated with apical toxicological endpoints and transcriptional changes in the liver and kidney. A benchmark response of one standard deviation was used to model all endpoints.

Results: Several clinical pathology and organ weight measurements showed dose-related changes from which BMD values were calculated. In male rats, the effects included significantly decreased total thyroxine concentration, increased absolute liver weight, increased relative liver weight, and decreased total triiodothyronine concentration. The BMDs and benchmark dose lower confidence limits (BMD_{LS}) were 7.264 (5.024), 8.492 (5.426), 16.251 (8.358), and 19.107 (7.426), respectively. In female rats, there were no apical endpoints for which a BMD value could be reliably estimated. Average PFHxSAm plasma concentrations at 2 and 24 hours postdose were lower in male rats than in female rats. Half-lives estimated using the two time points were longer in female rats (78.2 and 25.6 hours for the 4 and 37 mg/kg groups, respectively) than in male rats (40.1 and 15.1 hours for the 4 and 37 mg/kg groups, respectively).

In the liver of male and female rats, no Gene Ontology biological process or individual genes had BMD median values below the lower limit of extrapolation (<0.050 mg/kg). The most sensitive gene sets in male rats for which a reliable estimate of the BMD could be made were negative regulation of myeloid cell differentiation and regulation of cytokine production with median BMDs of 0.520 and 0.750 mg/kg and median BMD_{LS}s of 0.160 and 0.186 mg/kg, respectively. The most sensitive gene sets in female rats for which a reliable estimate of the BMD could be made were phenol-containing compound metabolic process and carboxylic acid catabolic process with median BMDs of 11.677 and 12.316 mg/kg and median BMD_{LS} of 5.931and 8.410 mg/kg, respectively. The most sensitive upregulated genes in male rats with reliable BMD estimates included *Gsta2*, *Gsta5*, *Crot*, *Slc27a2*, *Acaa1a*, and *Acaa1b* with BMDs (BMD_{LS}) of 5.725 (1.686), 5.725 (1.686), 7.423 (5.757), 7.622 (5.499), 8.417 (7.129), and 8.417 (7.129) mg/kg, respectively. The most sensitive downregulated genes in male rats with reliable BMD estimates were *Egr1*, *Zfp354a*, *Tsku*, and *Cyp7a1* with BMDs (BMD_{LS}) of 0.750 (0.186), 0.835 (0.271), 1.384 (0.541), and 5.721 (0.985) mg/kg, respectively. In female rats, the most sensitive upregulated genes with reliable BMD estimates included *Dao*, *Ephx2*, *Ehhadh*, *Cyp2b1*, *Loc108348266*/*Cyp2b1*, *Cyp2c6v1*, *Loc100911718*, and *Ech1* with BMDs (BMD_{LS}) of 6.134 (2.436), 6.441 (2.664), 7.300 (5.266), 7.456 (5.106), 7.456 (5.106), 9.829 (7.252), 9.829 (7.252), and 9.874 (6.591) mg/kg, respectively. The most sensitive downregulated genes in female rats

with reliable BMD estimates were *A2m* and *Loc100911545*/*A2m*, both with a BMD (BMD_L) of 1.163 (0.179) mg/kg.

In the kidney of male and female rats, no Gene Ontology biological process or individual genes had BMD median values below the lower limit of extrapolation (<0.050 mg/kg). The most sensitive gene sets in male rats for which a reliable estimate of the BMD could be made were fat cell differentiation and ER-nucleus signaling pathway, both with a median BMD of 8.745 mg/kg and with median BMD_Ls of 5.224 and 5.589 mg/kg, respectively. The most sensitive gene sets in female rats for which a reliable estimate of the BMD could be made were regulation of cell division, chromosome segregation, and cell division with median BMDs of 10.324, 11.921, and 11.921 mg/kg and median BMD_Ls of 7.461, 8.348, and 8.348 mg/kg, respectively. The most sensitive upregulated genes in male rats with reliable BMD estimates included *Insig1*, *Srebf1, Fads1*, *Ppard*, *Decr1*, *Acot2*, *Acaa1a*, *Acaa1b*, and *Fasn* with BMDs (BMD_Ls) of 7.612 (5.589), 8.745 (5.224), 9.357 (6.123), 9.934 (5.754), 12.862 (10.721), 13.201 (10.994), 13.398 (11.228), 13.398 (11.228), and 13.486 (11.223) mg/kg, respectively. One gene, *Loc100911814*/*Spink1l*, was downregulated with a BMD (BMD_L) of 0.510 (0.212) mg/kg. In female rats, the most sensitive upregulated genes with reliable BMD estimates included *Cdca3*, *Pck1*, *Ube2t*, *Srebf1*, *Ckap2*, *Lilra3*, *Lilrb3l*, and *Acaa1a* with BMDs (BMD_Ls) of 2.619 (0.978), 5.515 (1.341), 10.991 (7.866), 11.236 (4.944), 12.122 (8.470), 17.020 (10.650), 17.020 (10.650), and 17.682 (14.617) mg/kg, respectively. The most sensitive downregulated genes in female rats with reliable BMD estimates were *Slc10a1* and *Cyp2c24* with BMDs (BMD_Ls) of 7.968 (6.075) and 10.565 (7.636) mg/kg, respectively.

Summary: Taken together, in male rats, the most sensitive gene set BMD (BMD_L) median, individual gene BMD (BMD_L), and apical endpoint BMD (BMD_L) values that could be reliably determined occurred at 0.520 (0.160), 0.510 (0.212), and 7.264 (5.024) mg/kg, respectively. In female rats, the most sensitive gene set BMD (BMD_L) median and individual gene BMD (BMD_L) values that could be reliably determined occurred at 10.324 (7.461) and 1.163 (0.179) mg/kg, respectively. There were no apical endpoints in female rats for which a BMD value could be reliably estimated.

Background

Perfluorohexanesulfonamide (PFHxSAm) (CASRN: 41997-13-1, U.S. Environmental Protection Agency [EPA] Chemical Dashboard: DTXSID50469320,[1] PubChem CID: 11603678,[2] European Committee Number: 816-398-1[3]) is a member of the per- and polyfluoroalkyl class of compounds that are associated with numerous toxicological effects.[4] There is widespread human exposure to this class of compounds.[5; 6] The predicted upper 95th percentile human exposure to PFHxSAm is 0.0000563 mg/kg body weight/day.[7] A review of the existing literature failed to identify any in vivo toxicological information on PFHxSAm, and according to the EPA Chemical Dashboard, no quantitative risk assessment values or quantitative hazard values exist for this test article.[8] Publicly available information on PFHxSAm can be found in PubChem[2] and the EPA Chemical Dashboard.[1]

Recent studies have demonstrated that short-term in vivo gavage studies coupled with transcriptomics on select target organs can be used to estimate a biological potency that provides a reasonable approximation of toxicological potency in long-term guideline toxicological assessments.[9] To estimate biological potency and gain insight into the nature of biological changes elicited by PFHxSAm, the National Institute of Environmental Health Sciences performed a short-term in vivo biological potency study of male and female Sprague Dawley (Hsd:Sprague Dawley® SD®) rats. The results of this study are presented in this report.

Materials and Methods

Study Design

Male and female Sprague Dawley (Hsd:Sprague Dawley® SD®) rats were obtained from Envigo (Haslett, MI). On receipt, the rats were 6–7 weeks of age. Animals were quarantined for a minimum of 10 days and then randomly assigned to 1 of 10 dose groups. The rats in each dose group were then administered perfluorohexanesulfonamide (PFHxSAm) in acetone:corn oil (1:99) by gavage for 5 consecutive days (study days 0–4) at a dose level of 0, 0.15, 0.5, 1.4, 4, 12, 37, 111, 333, or 1,000 mg/kg body weight (mg/kg). There were 5 rats per sex in each dosed group and 10 per sex in the vehicle control group; an additional 3 rats per sex were added to the 4 and 37 mg/kg groups for internal dose assessment. Dosage volume was 5 mL/kg body weight and was based on each animal's most recent body weight. Euthanasia, blood/serum collection, and tissue sample collection were completed on study day 5, the day following the final administration of the test article. Blood was also collected from animals dedicated for internal dose assessment at 2 and 24 hours following the last dose administered on study day 4. Animal identification numbers and FASTQ data file names for each animal are presented in Appendix B.

Dose Selection Rationale

Dose selection was informed by a median lethal dose (LD_{50}) prediction from the OPEn structure-activity/property Relationship App (OPERA),[10; 11] which estimated 263 mg/kg/day with an uncertainty range of 131–525 mg/kg/day. Further, an estimated point of departure of 35 mg/kg/day with an uncertainty range of 0.9–916 mg/kg/day was provided by the U.S. Environmental Protection Agency (EPA).[12] To be certain that a 5-day maximum tolerated dose was achieved, in addition to identifying a minimum biological effect level dose, a top dose of 1,000 mg/kg/day was chosen, and approximately half-log dose spacing of nine lower dose levels, including a vehicle control, was selected to carry out the study.

Chemistry

PFHxSAm was obtained from SynQuest Laboratories, Inc. (Alachua, FL; lot Q156-19). The identity of the chemical was confirmed by fluorine nuclear magnetic resonance (^{19}F NMR) spectroscopy and by gas chromatography with mass spectrometry (GC/MS). The NMR spectrum was consistent with the structure of PFHxSAm, and GC/MS showed two isomeric peaks for PFHxSAm. Purity (95%; five impurities) of the chemical was assessed by GC/MS. Bulk chemical was stored at room temperature.

Dose formulations were prepared in 1% acetone in corn oil at 0 (vehicle control), 0.03, 0.10, 0.28, 0.80, 2.4, 7.4, 22.2, 66.6, and 200 mg/mL. The preadministration concentration of test article in the vehicle was analyzed using GC with flame ionization detection. The 0.03, 0.10, and 0.80 mg/mL formulations were 30.0%, 11.2%, and 14.3% above their target concentrations, respectively. The 200 mg/mL formulation was 16.5% below the target concentration. All other formulations were within 10% of their respective target concentration. Formulation stability was confirmed using a 0.10 mg/mL formulation for up to 15 days at room temperature. Homogeneity was confirmed using a 200 mg/mL formulation. All chemistry activities were conducted by RTI International (Research Triangle Park, NC).

Clinical Examinations and Sample Collection

Clinical Observations

All rats were observed twice daily for signs of mortality or moribundity. Formal (out of cage) clinical observations were performed daily.

Body and Organ Weights

Animals were weighed during quarantine for randomization on the first day of dosing (study day 0) and on the day of necropsy (study day 5). A gross necropsy was performed on all rats that died spontaneously or were humanely euthanized due to moribund condition. During necropsy for all animals, the heart, liver, and kidneys were removed, and organ weights were recorded; bilateral organs were weighed separately.

Clinical Pathology

Animals were euthanized in random order by CO_2/O_2 (70%/30%) anesthesia 1 day after the final day of dosing. Blood samples were collected from each sex within a 1-hour window and were taken via vena cava or aorta. Blood was collected into tubes containing K_3 EDTA (tripotassium ethylenediaminetetraacetic acid) for hematology analysis and into tubes void of anticoagulant for serum chemistry and thyroid hormone measurements. The following hematology parameters were measured on an Advia® 120 Hematology Analyzer (Siemens Medical Solutions USA, Inc., Malvern, PA): erythrocyte count, hemoglobin, hematocrit, mean cell volume, mean cell hemoglobin, mean cell hemoglobin concentration, white blood cell count and differential, reticulocyte count, platelet count, and nucleated erythrocyte count. Manual hematocrit was determined using a microcentrifuge and capillary reader. Blood smears were prepared, and qualitative evaluation of cellular morphology was performed per study protocol. The following clinical chemistry parameters were measured on a Roche cobas® c501 Chemistry Analyzer (Roche Diagnostics, Indianapolis, IN): alanine aminotransferase (ALT), albumin, alkaline phosphatase (ALP), aspartate aminotransferase (AST), total bile acids, total bilirubin, direct bilirubin, cholesterol, creatine kinase, creatinine, glucose, sorbitol dehydrogenase (SDH), total protein, triglycerides, and urea nitrogen. Globulin, albumin/globulin (A/G) ratio, and indirect bilirubin were calculated based on direct measurements (e.g., indirect bilirubin = total bilirubin − direct bilirubin). Serum concentrations for thyroid stimulating hormone (TSH) and free thyroxine (fT4) were determined by immunoassay using commercially available immunoassay kits from EMD Millipore Corporation (Billerica, MA) for TSH and Biomatik Corporation (Kitchener, Ontario, Canada) for fT4. Serum concentrations of total thyroxine (total T4) and total triiodothyronine (total T3) were determined using a validated method described elsewhere.[13] Individual animal and summary clinical chemistry, hematology, and hormonal data are available in Appendix F.

Internal Dose Assessment

A screening level assessment of the internal dose was performed to determine whether the test chemical had bioaccumulative properties (i.e., if the half-life was >24 hours). Blood was collected from animals dedicated for internal dose assessment in the 4 and 37 mg/kg groups at 2 and 24 hours following the last dose administered on study day 4. At 2 hours postdose, blood was collected from the jugular vein of unanesthetized animals. At 24 hours postdose (study

day 5), blood was collected from all study animals and dedicated internal dose assessment animals from the vena cava or abdominal aorta while animals were anesthetized with CO_2/O_2 (70%/30%). Blood was collected into tubes containing K_3 EDTA and kept on wet ice until plasma isolation, within 2 hours of collection. Samples were stored frozen (−85°C to −60°C) until analysis as described in Appendix A.

Transcriptomics

Sample Collection for Transcriptomics

Within 5 minutes of euthanasia, samples from the left liver lobe and right kidney were collected from all study animals for transcriptomic analysis. Half of the left liver lobe and half of the right kidney were processed for RNA isolation. Approximately 250 mg of each tissue was cut into small pieces (approximately 5 mm^3) and placed into cryotubes containing RNA*later*™. The tissue samples were stored at 2°C to 8°C overnight. The RNA*later*™ was then removed and the samples were stored in a −85°C to −60°C freezer until processed for RNA isolation.

RNA Isolation, Library Creation, and Sequencing

RNA isolation was performed on tissue samples preserved in RNA*later*™. Tissues were homogenized in QIAzol buffer (Qiagen Inc., Valencia, CA) using the TissueLyser II bead-beating system followed by RNA extraction using the Rneasy 96 QIAcube HT kits (Cat# 74171, Qiagen Inc., Valencia, CA) with a DNA digestion step. The concentration and purity of all isolated samples were determined from absorbency readings taken at 260 and 280 nm using a NanoDrop ND-8000 Spectrophotometer (NanoDrop Technologies, Wilmington, DE). The readings accurately determined the concentration of each sample while ensuring that an acceptable purity (A_{260}/A_{280} ratio) between 1.80 and 2.20 was achieved. After quantification, RNA was stored at −70°C ± 10°C until further processing.

One microliter of each RNA sample (500–660 ng/µL) was hybridized with the S1500+ beta detector oligo pool mix (2 µL per sample) using the following thermocycler settings: 10 minutes at 70°C, followed by a gradual decrease to 45°C over 49 minutes, and ending with a 45°C hold for 1 minute. Hybridization was followed by nuclease digestion (24 µL nuclease mix addition followed by 90 minutes at 37°C), ligation (24 µL ligation mix addition followed by 60 minutes at 37°C), and heat denaturation (at 80°C for 15 minutes). Ten microliters of each ligation product were then transferred to a 96-well polymerase chain reaction (PCR) amplification microplate with 10 µL of PCR mix per well. Through 25 cycles of amplification, well-specific "barcoded" primer pairs were introduced to templates. Five microliters of the PCR amplification products from each well were then pooled into a single sequencing library. The TempO-Seq library was then processed with a PCR clean-up kit (Machery-Nagel, Mountain View, CA) prior to sequencing. Sequencing was performed using a 50-cycle single-end read flow cell on a HiSeq 2500 Sequencing System (Illumina, San Diego, CA). Processing of sequencing data was conducted using Illumina's BCL2FASTQ software employing default parameter settings.

Sequence Data Processing

FASTQ files of TempO-Seq reads were aligned to the probe sequences from the target platform using Bowtie version 1.2.2[14] with the following parameters: -v 3 -k 1 -m 1 --best --strata. This configuration allows up to three mismatches and reports the single best alignment. After

alignment, the total sequenced reads, the percentage of reads aligning to the platform manifest, the alignment rate, and the percentage of expressed probes (≥5 reads per probe) were calculated for each sample.

Sequencing Quality Checks and Outlier Removal

Samples were flagged for values below the following thresholds: sequencing depth <300 K, total alignment rate <40%, unique alignment rate <30%, number of aligned reads <300 K, or percentage of probes with at least five reads <50%. Filtering on the percentage of expressed probes eliminates biased samples for which the sequenced reads only reflect a small portion of the measured transcriptome. In addition, FastQC was run on all samples to ensure adequate per base quality and per base N content, where N represents bases that could not be identified. All PFHxSAm samples passed the criteria mentioned above.

Principal component, hierarchical cluster, and inter-replicate correlation analyses were performed. These analyses highlighted one outlier liver sample, which was removed before downstream analysis. The final sample counts that were used for benchmark dose (BMD) analysis of the transcriptomics data are shown in Table 1.

Table 1. Final Sample Counts for Benchmark Dose Analysis of the Transcriptomics Data

	0 mg/kg	0.15 mg/kg	0.5 mg/kg	1.4 mg/kg	4 mg/kg	12 mg/kg	37 mg/kg	111 mg/kg	333 mg/kg	1,000 mg/kg
Male										
Liver	10	5	5	5	5	5	5	5	–[a]	–
Kidney	10	5	5	5	5	5	5	5	–	–
Female										
Liver	10	4	5	5	5	5	5	5	–	–
Kidney	10	5	5	5	5	5	5	5	–	–

[a]All male and female 333 and 1,000 mg/kg rats were found dead or moribund and euthanized by study day 1. Samples from these two dosed groups were not included in the sequencing.

Data Normalization

The aligned read counts for attenuated probes were properly readjusted to calculate unattenuated equivalent counts using the attenuation factors provided in the platform manifest. To account for between-sample sequencing depth variation, unattenuated read counts were normalized at the probe level by applying reads per million normalization. A pseudo-read-count of 1.0 was added to each normalized expression value, and then the values were log2 transformed to complete the normalization. Principal component-based visualizations of the final expression data set used from modeling are available in Appendix C.

Data Analysis

Statistical Analysis of Body Weights, Organ Weights, and Clinical Pathology

Two approaches were employed to assess the significance of pairwise comparisons between dosed and vehicle control groups in the analysis of continuous variables. Organ and body weight

data, which have approximately normal distributions, were analyzed using the parametric multiple comparison procedures of Williams[15; 16] and Dunnett.[17] Clinical pathology data, which typically have skewed distributions, were analyzed using the nonparametric multiple comparison methods of Shirley[18] and Dunn.[19] The Jonckheere test[20] was used to assess the significance of dose-response trends and to determine whether a trend-sensitive test (Williams or Shirley test) was more appropriate for pairwise comparisons than a test that assumes no monotonic dose response (Dunnett or Dunn test). Trend-sensitive tests were used when the Jonckheere test was significant at $p \leq 0.01$.

Prior to analysis, values identified by the outlier test of Dixon and Massey[21] were examined by National Institute of Environmental Health Sciences (NIEHS) staff. Values from animals suspected of illness due to causes other than experimental exposure and values that the laboratory indicated as inadequate due to measurement problems were eliminated from the analysis.

A no-observed-effect level (NOEL) was identified as the highest dose not showing a significant ($p \leq 0.05$) pairwise difference relative to the vehicle control group. A lowest-observed-effect level (LOEL) was identified as the lowest dose demonstrating a significant ($p \leq 0.05$) pairwise difference relative to the vehicle control group. Throughout the results section for apical endpoints, interpretation of BMDs is made in relationship to NOEL and LOEL values for specific endpoints, as defined here, and are not meant to reflect an overall study NOEL or LOEL.

Benchmark Dose Analysis of Body Weights, Organ Weights, and Clinical Pathology

Clinical pathology, body weight, and organ weight endpoints that exhibited a significant trend and pairwise test were submitted in batch for automated BMD modeling analysis. For body weight, the BMD and benchmark dose lower confidence limit (BMD_L) were presented as not determined when there were no significant results. BMD modeling and analysis was conducted using a modification of Benchmark Dose Modeling Software (BMDS) version 2.7.0. Data sets were executed using the Python BMDS interface (https://pypi.python.org/pypi/bmds; version 0.11), which allows for batch processing of multiple data sets. Data for all endpoints submitted were continuous. A default benchmark response (BMR) of one standard deviation (relative to control) was used for all data sets. The following BMDS 2.7.0 models were used to model the means of the data sets:

- Linear
- Polynomial 2°, 3°, 4°, 5°, 6°, 7°, 8°
- Power
- Hill
- Exponential M2, M3, M4, M5

Multiple versions of the polynomial model were executed, from a polynomial of degree 2 to a polynomial of degree equal to the number of dose groups minus 1 (e.g., if a data set had five dose groups, a 2°, 3°, and 4° polynomial model would be executed). Models were initialized using BMDS 2.7.0 model defaults, including restricting the power parameter of the power model and n-parameter of the Hill model to >1 and the beta parameters of the polynomial model to

positive or negative, depending on the mean response direction of the data set. For all models, either a constant or nonconstant variance model was selected as outlined in the EPA BMD technical guidance[22] and was implemented in the BMDS 2.7.0 software.

After model execution, BMDs were selected using the model recommendation procedures generally described in the EPA BMD technical guidance[22] and the automated decision logic described in Wignall et al.[23] and summarized in Appendix D, Table D-1. Models were placed into one of four possible bins, depending on the results and the bin recommendation logic:

(1) **Failure:** model did not successfully complete

(2) **Nonviable model (NVM):** model successfully completed but failed acceptability criteria

(3) **Not reportable (NR):** model is identified and meets all acceptability criteria with the exception of the estimated BMD being below the lower limit of extrapolation (<1/3 the lowest nonzero dose tested); BMD reported as <1/3 the lowest nonzero dose tested and BMD_L is not reportable

(4) **Viable model:** candidate for recommended model without warning

If only one model was in the viable model bin, it was selected as the best-fitting model. If the viable bin had more than one model, consistent with EPA guidance,[22] either the model with the lowest Akaike information criterion (AIC) or lowest BMD_L was selected. If the range of BMD_L values was sufficiently close (less than threefold difference), the AIC value was used; otherwise, the BMD_L value was used. If no model was recommended, no BMD was presented in the results. Details on the analysis criteria and decision tree are provided in Table D-1 and Figure D-1, respectively. To avoid effects of model extrapolation, BMD values derived from viable models that were threefold lower than the lowest nonzero dose tested were reported as <1/3 the lowest nonzero dose tested, and corresponding BMD_L values were not reported. Finally, all modeling results from apical data yielding a BMD were reviewed by a subject matter expert to determine the validity of the modeling results and potency estimates.

Benchmark Dose Analysis of Transcriptomics Data

The BMD analysis of the transcriptomic data was performed in accordance with the National Toxicology Program (NTP) best practices for genomic dose-response modeling as reviewed by an independent panel of experts in October 2017. These recommendations are described in the 2018 publication, *National Toxicology Program Approach to Genomic Dose Response Modeling*.[24]

Dose-response analyses of normalized gene expression data were performed using BMDExpress 2.30.0507 BETA (https://github.com/auerbachs/BMDExpress-2/releases). A trend test (the Williams trend test[15; 16] $p \leq 0.05$, 10,000 permutations) and fold change filter (1.5-fold change up or down relative to the vehicle control group for probe sets) were applied to the data set to remove probe sets demonstrating no response to chemical exposure from subsequent analysis. These filter criteria were empirically determined with the goal of balancing false discovery with reproducibility. The criteria are consistent with the MicroArray Quality Control recommendations to combine the nominal p value threshold with a fold change filter to maximize replicability of transcriptomic findings across labs.[25] The following dose-response models were fit to the probe sets that passed the trend test and fold change filter:

- Hill
- Power
- Linear
- Polynomial 2°
- Exponential M2, M3, M4, M5

All gene expression data analyzed in BMDExpress were log2 transformed, and thus nearly all probes (also known as detection oligos or DO) were assumed to exhibit constant variance across the doses. For this reason and for efficiency purposes, each model was run assuming constant variance. Lacking any broadly applicable guidance regarding the level of change in gene expression considered biologically significant, a BMR of one standard deviation (relative to the fit at control) was used in this study. This approach enables standardization of the BMR between apical endpoints and transcriptomic endpoints and provides a standard for use across multiple chemicals tested in this rapid screening paradigm. The expression direction (upregulated or downregulated) for each probe was determined by a trend test intrinsic to the model executables (provided by EPA) contained in BMDExpress.

To identify the best-fit model for each fitted probe, the AIC values for each fitted model were compared and the model with the lowest AIC was selected. The best model for each probe was used to calculate the BMD, BMD_L, and BMD upper confidence limit (BMD_U). The specific parameter settings, selected from the BMDExpress software when performing probe-level BMD analysis, were as follows: maximum iterations – 250, confidence level – 0.95, BMR factor – 1 (the multiplier of the standard deviation that defined the BMD), restrict power – no restriction, and constant variance – selected. The specific model selection setting in the BMDExpress software when performing probe set-level BMD analysis was as follows: best poly model test – lowest AIC, flag Hill model with "k" parameters – <1/3 the lowest nonzero dose tested, and best model selection with flagged Hill model – include flagged Hill model. The inclusion of the flagged models is a deviation from EPA BMD analysis guidance.[22] The justification for this deviation relates to subsequent use of the data in which the probe BMD values are grouped into gene sets from which a median BMD is derived. If the probes were removed from the analysis or forced to another model, the probe might not be counted in the gene set analysis and could lead to loss of "active" gene sets. Importantly, most of the probes that produce flagged Hill models show highly potent responses and should therefore be counted in the analysis.

To perform Gene Ontology (GO; annotation accession date: 07/15/2020) gene set analysis, only GO terms with ≥10 and ≤250 annotated genes measured on the gene expression platform were considered. Before sorting genes into the GO terms, the best-fit model for each probe was subjected to a filtering process to remove those probes (1) with a BMD greater than the highest dose tested, (2) that mapped to more than one gene, (3) that had a global goodness-of-fit p value ≤0.1, and (4) with a BMD_U/BMD_L ratio >40. GO terms that were at least 5% populated and contained three genes that passed the criteria mentioned above were considered "active" (i.e., responsive to chemical exposure). For this report, GO terms populated with identical sets of differentially expressed genes were filtered to limit redundancy in reporting based on the following selection criteria: (1) highest percentage populated and (2) most specific/highest GO level. Redundant GO terms failing to differentiate on the basis of these criteria were retained and reported. A complete list of "active" GO terms can be found in Appendix F. To avoid effects of

model extrapolation, GO terms exhibiting BMD values below the lower limit of extrapolation (<1/3 the lowest nonzero dose tested) were reported as <1/3 the lowest nonzero dose tested and corresponding BMD_L and BMD_U values were not reported.

To perform Individual Gene Analysis, the best-fit model for each probe was subjected to a filtering process to remove those probes (1) with a BMD greater than the highest dose tested, (2) that mapped to more than one gene, (3) that had a global goodness-of-fit p value ≤0.1, or (4) with a BMD_U/BMD_L ratio >40. For genes that had more than one probe represented on the platform and passed this filtering process, a median BMD was used to estimate the BMD, BMD_L, and BMD_U values. To ensure only genes with a robust response were assessed for potency, genes with probes that had a median fold change <|2| were removed prior to reporting. A complete list of genes and their corresponding metrics can be found in Appendix F. To avoid effects of model extrapolation, genes exhibiting BMD values below the lower limit of extrapolation (<1/3 the lowest nonzero dose tested) were reported as <1/3 the lowest nonzero dose tested and corresponding BMD_L and BMD_U values were not reported.

A summary of the BMDExpress gene expression analysis pipeline used in this study is shown in Figure D-2.

Empirical False Discovery Rate Determination for Genomic Dose-response Modeling

The genomic dose-response analysis pipeline is a complex multistep process with multiple modeling steps and parameter variables. Because of this complexity, traditional statistical models for determining false discovery rates for the genes and pathways are not straightforward to apply. To overcome this issue, an empirical false discovery rate was determined on the basis of the totality of the analysis pipeline. This was done through the evaluation of synthetic null data sets derived from vehicle control data from four short-term repeat dose toxicogenomic studies including PFHxSAm (each with 10 vehicle control samples). The other toxicogenomic studies, which are reported in separate NIEHS reports, are of 6:1 fluorotelomer alcohol,[26] 1,1,2,2-tetrahydroperfluoro-1-dodecanol,[27] and 2,3-benzofluorene.[28] Samples from all four studies were processed as a group and subjected to sequencing at the same time and were visually inspected to ensure there was no batch effect between the different studies.

To create synthetic null data for a given group (tissue per sex combination), up to 40 vehicle control samples from the original studies (10 replicates × 4 chemicals) were used to generate the data sets, with outliers excluded from the analysis. Each computationally generated sample was created by mixing two randomly selected vehicle control samples via a weighted average approach through which weights were obtained from random uniform (0,1) distribution. A total of 55 samples (10 vehicle control samples + 45 dosed samples [9 doses × 5 replicates]) were computationally generated per data set and assigned doses spaced by approximately half-log. A total of 20 data sets were generated per group (i.e., 20 data sets each for female kidney, male kidney, female liver, and male liver) and analyzed using both the individual gene-level and GO biological process (gene set) analysis pipeline employed to analyze the data from each study. The median empirical false discovery rates across the 20 null sets in each group for gene-level analysis across each group were 0.037%, 0.037%, 0%, and 0% (female kidney, male kidney, female liver, and male liver, respectively). The median empirical false discovery rate for each of the 20 null data sets in each group using the GO biological process (gene set) level analysis was

0%. Details of the empirical false discovery rate analysis are available in Appendix C. The associated bm2 analysis file that is the basis of the empirical false discovery rate can be found in Appendix F.

Data Accessibility

Primary and analyzed data used in this study are available to the public at https://doi.org/10.22427/NIEHS-DATA-NIEHS-10.[29]

Results

Animal Condition, Body Weights, and Organ Weights

Male and female rats administered 333 or 1,000 mg/kg body weight (mg/kg) of perfluorohexanesulfonamide (PFHxSAm) began exhibiting signs of overt toxicity on study day 1, which included red discharge from nose/snout and penis, clear or red discharge from eyes, labored breathing, pale appearance, salivation, hunched posture, prone positioning, and lethargy (Appendix F). In the 333 mg/kg group, three male rats and four female rats were found dead on study day 1, and the remaining rats were moribund and euthanized at that time due to severe toxicity. In the 1,000 mg/kg day group, one male rat was found dead on study day 0, four male rats and four female rats were found dead on study day 1, and the remaining female rat was moribund and euthanized at that time. Rats in the 0, 0.15, 0.5, 1.4, 4, 12, 37, and 111 mg/kg groups did not exhibit signs of overt toxicity, and all survived to study termination. No significant changes in terminal body weight for male or female rats occurred with exposure to PFHxSAm (Table 2).

In male rats at study termination, a significant increase in absolute and relative liver weights occurred in dose groups ≥12 mg/kg; these endpoints had positive trends (Table 3). The benchmark doses (benchmark dose lower confidence limits)—BMDs (BMD_{LS})—for increased absolute and relative liver weights were 8.492 (5.426) and 16.251 (8.358) mg/kg, respectively. The BMDs for all organ weights were reviewed by a subject matter expert for anomalous modeling results (i.e., when the traditional statistics are notably different from the estimated BMD values). Significant trend and pairwise comparisons were not observed in absolute or relative heart, right kidney, or left kidney weights (Appendix F).

In female rats at study termination, there were no organ weights that exhibited significant trend and pairwise comparisons (Appendix F).

Table 2. Summary of Body Weights of Male and Female Rats Administered Perfluorohexanesulfonamide for Five Days

Study Day[a,b]	0 mg/kg	0.15 mg/kg	0.5 mg/kg	1.4 mg/kg	4 mg/kg	12 mg/kg	37 mg/kg	111 mg/kg	333 mg/kg	1,000 mg/kg	BMD_{1Std} (mg/kg)	BMD_{L1Std} (mg/kg)
Male												
n	10	5	5	5	5	5	5	5	5	4[c]	NA	NA
0	296.5 ± 4.4	297.3 ± 4.5	295.9 ± 1.6	303.7 ± 5.0	292.6 ± 3.8	304.1 ± 3.0	293.2 ± 4.0	298.5 ± 6.0	298.6 ± 3.4	293.8 ± 4.5	ND	ND
5	311.0 ± 5.2	314.0 ± 5.1	315.5 ± 1.4	320.1 ± 4.8	308.2 ± 4.4	325.9 ± 4.7	308.6 ± 4.2	308.6 ± 3.9	–[d]	–	ND	ND
Female												
n	10	5	5	5	5	5	5	5	5	5	NA	NA
0	210.1 ± 5.4	209.1 ± 6.6	206.7 ± 3.9	205.2 ± 4.2	212.9 ± 7.1	206.8 ± 3.9	203.6 ± 4.6	207.0 ± 3.9	204.9 ± 4.4	203.6 ± 4.5	ND	ND
5	221.0 ± 5.4	215.4 ± 7.5	211.0 ± 4.0	213.0 ± 6.5	219.0 ± 7.4	216.3 ± 6.2	208.2 ± 5.5	213.2 ± 4.0	–	–	ND	ND

BMD_{1Std} = benchmark dose corresponding to a benchmark response set to one standard deviation from the mean; BMD_{L1Std} = benchmark dose lower confidence limit corresponding to a benchmark response set to one standard deviation from the mean; NA = not applicable; ND = not determined.
[a]Data are displayed as mean ± standard error of the mean; body weight data are presented in grams.
[b]Statistical analysis performed by the Jonckheere (trend) and Williams or Dunnett (pairwise) tests.
[c]One male rat was found dead on study day 0.
[d]All male and female 333 and 1,000 mg/kg rats were found dead or moribund and euthanized by study day 1.

Table 3. Summary of Liver Weights of Male Rats Administered Perfluorohexanesulfonamide for Five Days

Endpoint[a,b,c]	0 mg/kg	0.15 mg/kg	0.5 mg/kg	1.4 mg/kg	4 mg/kg	12 mg/kg	37 mg/kg	111 mg/kg	333 mg/kg	1,000 mg/kg	BMD_{1Std} (mg/kg)	BMD_{L1Std} (mg/kg)
n	10	5	5	5	5	5	5	5	–[d]	–	NA	NA
Terminal Body Wt. (g)	311.0 ± 5.2	314.0 ± 5.1	315.5 ± 1.4	320.1 ± 4.8	308.2 ± 4.4	325.9 ± 4.7	308.6 ± 4.2	308.6 ± 3.9	–	–	ND	ND
Liver												
Absolute (g)	11.48 ± 0.31**	12.00 ± 0.37	12.31 ± 0.30	12.48 ± 0.35	11.80 ± 0.35	13.14 ± 0.41**	12.75 ± 0.30**	14.31 ± 0.11**	–	–	8.492	5.426
Relative (mg/g)[e]	36.88 ± 0.52**	38.21 ± 0.78	39.03 ± 0.85	39.01 ± 1.22	38.26 ± 0.77	40.28 ± 0.78**	41.33 ± 1.00**	46.42 ± 0.86**	–	–	16.251	8.358

Statistical significance for a dosed group indicates a significant pairwise test compared to the vehicle control group. Statistical significance for the vehicle control group indicates a significant trend test.
**Statistically significant at $p \leq 0.01$.
BMD_{1Std} = benchmark dose corresponding to a benchmark response set to one standard deviation from the mean; BMD_{L1Std} = benchmark dose lower confidence limit corresponding to a benchmark response set to one standard deviation from the mean; NA = not applicable; ND = not determined.
[a]Descriptions of organ weight endpoints and changes are provided in Appendix E.
[b]Data are displayed as mean ± standard error of the mean.
[c]Statistical analysis performed by the Jonckheere (trend) and Williams or Dunnett (pairwise) tests.
[d]All male and female 333 and 1,000 mg/kg rats were found dead or moribund and euthanized by study day 1.
[e]Relative organ weights (organ weight-to-body weight ratios) are given as mg organ weight/g body weight.

Clinical Pathology

In male rats, cholesterol concentration exhibited significant trend and pairwise comparisons. In female rats, both aspartate aminotransferase and sorbitol dehydrogenase activities exhibited significant trend and pairwise comparisons. Although a BMD was estimated for each of these endpoints, these values were much lower (approximately 75- to 230-fold, 140- to 430-fold, and 25- to 80-fold for cholesterol concentration in male rats, aspartate aminotransferase activity in female rats, and sorbitol dehydrogenase activity in female rats, respectively) than would be expected given the endpoint-specific no-observed-effect level (NOEL) and lowest-observed-effect level (LOEL) values, suggesting that the BMD estimate did not accurately reflect the true potency of the effect and was likely an anomalous product of the BMD modeling approach (Table 4). The BMDs for all clinical pathology endpoints were reviewed by a subject matter expert for anomalous modeling results (i.e., when the traditional statistics are notably different from the estimated BMD values).

In male rats, neutrophil count had significant trend and pairwise comparisons. Although a BMD was estimated, its value was much lower (approximately 45- to 140-fold) than would be expected given the endpoint-specific NOEL and LOEL values, suggesting that the BMD estimate did not accurately reflect the true potency of the effect and was likely an anomalous product of the BMD modeling approach (Table 5)**.** In female rats, there was a negative trend and significant pairwise comparisons for the manual hematocrit in the ≥37 mg/kg groups; a BMD (BMD_L) was not determined because no viable model was available.

In male rats, both total thyroxine (total T4) and total triiodothyronine (total T3) concentrations had a negative trend with significant pairwise comparisons in the ≥12 mg/kg and 111 mg/kg groups, respectively (Table 6). The BMDs (BMD_{LS}) for decreased total T4 and decreased total T3 were 7.264 (5.024) and 19.107 (7.426) mg/kg, respectively. In female rats, total T4 concentration had significant trend and pairwise comparisons. Although a BMD was estimated, its value was much lower (approximately 30- to 90-fold) than would be expected given the endpoint-specific NOEL and LOEL values, suggesting that the BMD estimate did not accurately reflect the true potency of the effect and was likely an anomalous product of the BMD modeling approach.

Table 4. Summary of Select Clinical Chemistry Data for Male and Female Rats Administered Perfluorohexanesulfonamide for Five Days

Endpoint[a,b]	0 mg/kg	0.15 mg/kg	0.5 mg/kg	1.4 mg/kg	4 mg/kg	12 mg/kg	37 mg/kg	111 mg/kg	333 mg/kg	1,000 mg/kg	BMD_{1Std} (mg/kg)	BMD_{L1Std} (mg/kg)
Male												
n	9[c]	5	5	5	5	5	5	5	–[d]	–	NA	NA
Cholesterol (mg/dL)	103.3 ± 4.4**	102.2 ± 4.0	123.0 ± 12.6	115.0 ± 12.1	109.2 ± 4.5	108.4 ± 6.3	90.2 ± 4.8	79.8 ± 4.0**	–	–	0.484[e]	0.225[e]
Female												
n	10	5	5	5	5	5	5	5	–	–	NA	NA
Aspartate Aminotransferase (U/L)	82.20 ± 1.88**	80.60 ± 1.21	72.40 ± 2.62	74.40 ± 3.08	77.60 ± 4.50	82.00 ± 2.88	77.80 ± 4.42	69.60 ± 1.57**	–	–	0.256[e]	0.11[e]
Sorbitol Dehydrogenase (IU/L)	11.9 ± 0.9**	11.8 ± 0.7	9.3 ± 0.5	10.1 ± 0.5	11.8 ± 1.0	11.8 ± 1.5	8.6 ± 0.4**	9.1 ± 0.4*	–	–	0.455[e]	0.264[e]

Statistical significance for a dosed group indicates a significant pairwise test compared to the vehicle control group. Statistical significance for the vehicle control group indicates a significant trend test.
*Statistically significant at $p \leq 0.05$; **$p \leq 0.01$.
BMD_{1Std} = benchmark dose corresponding to a benchmark response set to one standard deviation from the mean; BMD_{L1Std} = benchmark dose lower confidence limit corresponding to a benchmark response set to one standard deviation from the mean; NA = not applicable.
[a]Data are displayed as mean ± standard error of the mean.
[b]Statistical analysis performed by the Jonckheere (trend) and Shirley or Dunn (pairwise) tests.
[c]One sample in the indicated dose group was not received.
[d]All male and female 333 and 1,000 mg/kg rats were found dead or moribund and euthanized by study day 1.
[e]BMD values are much lower than would be expected given the lowest-observed-effect level and no-observed-effect level values, suggesting that the BMD estimates do not accurately reflect the true potency of the effect of these endpoints and are likely an anomalous product of the BMD modeling approach.

Table 5. Summary of Select Hematology Data for Male and Female Rats Administered Perfluorohexanesulfonamide for Five Days

Endpoint[a,b]	0 mg/kg	0.15 mg/kg	0.5 mg/kg	1.4 mg/kg	4 mg/kg	12 mg/kg	37 mg/kg	111 mg/kg	333 mg/kg	1,000 mg/kg	BMD_{1Std} (mg/kg)	BMD_{L1Std} (mg/kg)
Male												
n	6[c,d]	2[d]	4[e]	4[e]	5	3[f]	2[d]	4[e]	–[g]	–	NA	NA
Neutrophils (10^3/µL)	0.84 ± 0.12**	1.08 ± 0.22	0.85 ± 0.06	1.34 ± 0.16	1.54 ± 0.21	1.25 ± 0.19	1.23 ± 0.01	1.24 ± 0.16*	–	–	0.811[h]	0.305[h]
Female												
n	8[f]	5	5	3[f]	4[e]	4[e]	4[e]	5	–	–	NA	NA
Manual Hematocrit (%)	44.6 ± 0.5**	47.4 ± 2.7	45.0 ± 0.7	44.3 ± 0.9	44.3 ± 0.5	43.5 ± 0.6	43.0 ± 0.0*	42.6 ± 0.7*	–	–	NVM	NVM

Statistical significance for a dosed group indicates a significant pairwise test compared to the vehicle control group. Statistical significance for the vehicle control group indicates a significant trend test.
*Statistically significant at $p \leq 0.05$; **$p \leq 0.01$.
BMD_{1Std} = benchmark dose corresponding to a benchmark response set to one standard deviation from the mean; BMD_{L1Std} = benchmark dose lower confidence limit corresponding to a benchmark response set to one standard deviation from the mean; NA = not applicable; NVM = nonviable model.
[a]Data are displayed as mean ± standard error of the mean.
[b]Statistical analysis performed by the Jonckheere (trend) and Shirley or Dunn (pairwise) tests.
[c]One sample in the indicated dose group was not received.
[d]Three samples from each of the indicated dose groups had a clot present and were not analyzed.
[e]One sample from each of the indicated dose groups had a clot present and was not analyzed.
[f]Two samples from each of the indicated dose groups had a clot present and were not analyzed.
[g]All male and female 333 and 1,000 mg/kg rats were found dead or moribund and euthanized by study day 1.
[h]BMD values are much lower than would be expected given the lowest-observed-effect level and no-observed-effect level values, suggesting that the BMD estimates do not accurately reflect the true potency of the effect of these endpoints and are likely an anomalous product of the BMD modeling approach.

Table 6. Summary of Select Hormone Data for Male and Female Rats Administered Perfluorohexanesulfonamide for Five Days

Endpoint[a,b]	0 mg/kg	0.15 mg/kg	0.5 mg/kg	1.4 mg/kg	4 mg/kg	12 mg/kg	37 mg/kg	111 mg/kg	333 mg/kg	1,000 mg/kg	BMD_{1Std} (mg/kg)	BMD_{L1Std} (mg/kg)
Male												
n	6[c]	3[d]	5	5	4[e]	4[e]	3[d]	5	–[f]	–	NA	NA
Total T3 (ng/dL)	52.550 ± 3.147**	55.767 ± 8.167	58.340 ± 5.567	51.040 ± 5.683	53.750 ± 5.446	49.425 ± 5.193	36.467 ± 5.102	24.160 ± 1.202**	–	–	19.107	7.426
Total T4 (µg/dL)	3.03 ± 0.29**	3.09 ± 0.58	2.73 ± 0.27	2.69 ± 0.33	2.95 ± 0.28	2.02 ± 0.34*	0.79 ± 0.17**	0.45 ± 0.04**	–	–	7.264	5.024
Female												
n	9[e]	4[e]	5	5	4[e]	4[e]	4[e]	5	–	–	NA	NA
Total T4 (µg/dL)	2.76 ± 0.15**	2.74 ± 0.31	3.41 ± 0.29	3.43 ± 0.24	2.62 ± 0.30	2.55 ± 0.21	1.84 ± 0.23*	1.06 ± 0.12**	–	–	0.417[g]	0.117[g]

Statistical significance for a dosed group indicates a significant pairwise test compared to the vehicle control group. Statistical significance for the vehicle control group indicates a significant trend test.

*Statistically significant at $p \leq 0.05$; **$p \leq 0.01$.

BMD_{1Std} = benchmark dose corresponding to a benchmark response set to one standard deviation from the mean; BMD_{L1Std} = benchmark dose lower confidence limit corresponding to a benchmark response set to one standard deviation from the mean; NA = not applicable; total T3 = total triiodothyronine; total T4 = total thyroxine.

[a]Data are displayed as mean ± standard error of the mean.

[b]Statistical analysis performed by the Jonckheere (trend) and Shirley or Dunn (pairwise) tests.

[c]Four samples in the indicated dose group did not have sufficient specimen volume available for analysis.

[d]Two samples in the indicated dose groups did not have sufficient specimen volume available for analysis.

[e]One sample in the indicated dose groups did not have sufficient specimen volume available for analysis.

[f]All male and female 333 and 1,000 mg/kg rats were found dead or moribund and euthanized by study day 1.

[g]BMD values are much lower than would be expected given the lowest-observed-effect level and no-observed-effect level values, suggesting that the BMD estimates do not accurately reflect the true potency of the effect of these endpoints and are likely an anomalous product of the BMD modeling approach.

Internal Dose Assessment

For the 4 and 37 mg/kg groups, PFHxSAm plasma concentrations were determined at 2 and 24 hours following the last dose administered on study day 4 to male and female rats. Average PFHxSAm concentrations are given in Table 7. In general, average plasma concentrations in female rats were higher than those in male rats. At 2 and 24 hours following administration to male and female rats—as the administered dose increased from 4 to 37 mg/kg (a ninefold increase)—there was a less-than-proportional increase (approximately four- and twofold, respectively) in the average PFHxSAm plasma concentration, suggesting changes in the absorption, distribution, metabolism, and excretion processes (e.g., lower absorption and/or induction of metabolism and clearance pathways) as the dose increased. Half-lives estimated using the data from these two time points were longer in female rats (78.2 and 25.6 hours for the 4 and 37 mg/kg groups, respectively) than in male rats (40.1 and 15.1 hours for the 4 and 37 mg/kg groups, respectively). The shorter plasma elimination half-lives estimated for the higher dosed group compared to the lower dosed group suggest induction of clearance pathways as the dose increases.

Table 7. Summary of Plasma Concentration Data for Male and Female Rats Administered Perfluorohexanesulfonamide for Five Days[a]

	4 mg/kg	37 mg/kg
n	3	3
Male		
2 Hours Postdose (ng/mL)	33.8 ± 4.43	137 ± 10.6
24 Hours Postdose (ng/mL)	23.1 ± 3.42	50.0 ± 19.4
Female		
2 Hours Postdose (ng/mL)	46.3 ± 5.96	184 ± 3.06
24 Hours Postdose (ng/mL)	38.1 ± 3.36	101 ± 3.08

If over 20% of the animals in a group are above the limit of detection, then half the limit of detection value is substituted for values that are below it.
[a]Data are displayed as mean ± standard error of the mean.

Apical Endpoint Benchmark Dose Summary

A summary of the calculated BMDs for each toxicological endpoint is provided in Table 8. The endpoint-specific LOEL and NOEL are included and could be informative for endpoints that lack a calculated BMD either because no viable model was available or because the estimated BMD was below the lower limit of extrapolation (<0.050 mg/kg).

Table 8. BMD, BMD_L, LOEL, and NOEL Summary for Apical Endpoints, Sorted by BMD or LOEL from Low to High

Endpoint	BMD_{1Std} (mg/kg)	BMD_{L1Std} (mg/kg)	LOEL (mg/kg)[a]	NOEL (mg/kg)	Direction of Change
Male					
Total Thyroxine	7.264	5.024	12	4	DOWN
Absolute Liver Weight	8.492	5.426	12	4	UP
Relative Liver Weight	16.251	8.358	12	4	UP
Total Triiodothyronine	19.107	7.426	111	37	DOWN
Cholesterol	UREP[b]	UREP[b]	**111**	37	–[b]
Neutrophils	UREP	UREP	**111**	37	–
Female					
Manual Hematocrit	NVM	NVM	**37**	12	DOWN
Sorbitol Dehydrogenase	UREP	UREP	**37**	12	–
Total Thyroxine	UREP	UREP	**37**	12	–
Aspartate Aminotransferase	UREP	UREP	**111**	37	–

BMD_{1Std} = benchmark dose corresponding to a benchmark response set to one standard deviation from the mean; BMD_{L1Std} = benchmark dose lower confidence limit corresponding to a benchmark response set to one standard deviation from the mean; LOEL = lowest-observed-effect level; NOEL = no-observed-effect level; UREP = unreliable estimate of potency is a label based on review by a subject matter expert and rejection of BMD modeling results; NVM = nonviable model, defined as a modeling result that does not meet prespecified fit criteria and hence is deemed unreliable.
[a]Values in bold text indicate the LOEL of endpoints for which a BMD could not be calculated.
[b]BMD values are much lower than would be expected given the endpoint-specific LOEL and NOEL values, suggesting that the BMD estimates do not accurately reflect the true potency of the effect of these endpoints and are likely an anomalous product of the BMD modeling approach.

Gene Set Benchmark Dose Analysis

Chemical-induced alterations in liver and kidney gene transcript expression were examined to determine those gene sets most sensitive to PFHxSAm exposure. To that end, BMD analysis of transcripts and gene sets (Gene Ontology [GO] biological process) was conducted to determine the potency of the chemical to elicit gene expression changes in the liver and kidney. This analysis used transcript-level BMD data to assess an aggregate score of gene set potency (median transcript BMD) and enrichment.

The “active” gene sets in the liver and kidney with the lowest BMD median values are shown in Table 9 and Table 10, respectively. The gene sets in Table 9 and Table 10 should be interpreted with caution from the standpoint of the underlying biological mechanism and any relationship to toxicity or toxic agents referenced in the GO term definitions. The data primarily should be considered a metric of potency for chemical-induced transcriptional changes (i.e., a concerted biological change) that could serve as a surrogate of estimated biological potency and, by extension, toxicological potency when more definitive toxicological data are unavailable.

No gene sets in the liver of male or female rats had estimated BMD median values <0.050 mg/kg. In male rats, the most sensitive GO biological processes for which a BMD value could be reliably calculated were negative regulation of myeloid cell differentiation (GO:0045638) and regulation of cytokine production (GO:0001817) with median BMDs

(BMD_{LS}) of 0.520 (0.160) and 0.750 (0.186) mg/kg, respectively. In female rats, the most sensitive GO biological processes for which a BMD value could be reliably calculated were phenol-containing compound metabolic process (GO:0018958) and carboxylic acid catabolic process (GO:0046395) with median BMDs (BMD_{LS}) of 11.677 (5.931) and 12.316 (8.410) mg/kg, respectively.

No gene sets in the kidney of male or female rats had estimated BMD median values <0.050 mg/kg. In male rats, the most sensitive GO biological processes for which a BMD value could be reliably calculated were fat cell differentiation (GO:0045444) and ER-nucleus signaling pathway (GO:0006984) with median BMDs (BMD_{LS}) of 8.745 (5.224) and 8.745 (5.589) mg/kg, respectively. In female rats, the most sensitive GO biological processes for which a BMD value could be reliably calculated were regulation of cell division (GO:0051302) with a median BMD (BMD_{L}) of 10.324 (7.461) mg/kg, and chromosome segregation (GO:0007059) and cell division (GO: 0051301), both with a median BMD (BMD_{L}) of 11.921 (8.348) mg/kg. The full list of affected gene sets in the liver and kidney of male and female rats can be found in Appendix F.

Table 9. Top 10 Liver Gene Ontology Biological Process Gene Sets Ranked by Potency of Perturbation, Sorted by Benchmark Dose Median[a]

Category Name	No. of Active Genes/ Platform Genes in Gene Set	% Gene Set Coverage	Active Genes	BMD_{1std} Median of Gene Set Transcripts (mg/kg)	Median BMD_{L1Std}–BMD_{U1Std} (mg/kg)	Genes with Changed Direction Up	Genes with Changed Direction Down
Male							
GO:0045638 negative regulation of myeloid cell differentiation	3/31	10%	*Zfp36*; *Pik3r1*; *Nfkbia*	0.520	0.160–2.885	0	3
GO:0001817 regulation of cytokine production	3/43	7%	*Zfp36*; *Hspb1*; *Egr1*	0.750	0.186–4.702	0	3
GO:0007611 learning or memory	4/79	5%	*Jun*; *Hmgcr*; *Fos*; *Egr1*	1.190	0.425–6.165	0	4
GO:0030178 negative regulation of Wnt signaling pathway	3/31	10%	*Tsku*; *Foxo3*; *Egr1*	1.384	0.541–4.702	0	3
GO:0007612 learning	3/43	7%	*Jun*; *Hmgcr*; *Fos*	1.631	0.663–7.629	0	3
GO:0006695 cholesterol biosynthetic process	3/21	14%	*Tm7sf2*; *Hsd17b7*; *Hmgcr*	1.631	0.663–7.629	0	3

Category Name	No. of Active Genes/ Platform Genes in Gene Set	% Gene Set Coverage	Active Genes	BMD_{1std} Median of Gene Set Transcripts (mg/kg)	Median BMD_{L1Std}–BMD_{U1Std} (mg/kg)	Genes with Changed Direction Up	Genes with Changed Direction Down
GO:0043409 negative regulation of MAPK cascade	3/51	6%	*Sirt3*; *Hmgcr*; *Dusp6*	2.380	0.663–8.829	1	2
GO:0014072 response to isoquinoline alkaloid	3/19	16%	*Fga*; *Egr1*; *Abcg2*	5.217	2.734–11.386	1	2
GO:0008203 cholesterol metabolic process	5/49	10%	*Tm7sf2*; *Hsd17b7*; *Hmgcr*; *Fgl1*; *Cyp7a1*	5.721	0.985–22.363	0	5
GO:0051412 response to corticosterone	3/27	11%	*Foxo3*; *Fos*; *Cdkn1a*	6.250	2.440–19.061	0	3
Female							
GO:0018958 phenol-containing compound metabolic process	4/31	13%	*Sult1b1*; *Srd5a1*; *Dao*; *Cyp2e1*	11.677	5.931–25.645	3	1
GO:0046395 carboxylic acid catabolic process	13/87	15%	*Gcdh*; *Ehhadh*; *Eci2*; *Eci1*; *Ech1*; *Decr1*; *Dao*; *Crat*; *Cpt2*; *Acox1*; *Acot4*; *Acot2*; *Acaa2*	12.316	8.410–24.399	12	1
GO:0044242 cellular lipid catabolic process	13/64	20%	*Gcdh*; *Ehhadh*; *Eci2*; *Eci1*; *Ech1*; *Decr1*; *Crat*; *Cpt2*; *Apoa2*; *Angptl3*; *Acox1*; *Acot2*; *Acaa2*	13.636	10.423–28.083	12	1
GO:0009062 fatty acid catabolic process	11/42	26%	*Gcdh*; *Ehhadh*; *Eci2*; *Eci1*; *Ech1*; *Decr1*; *Crat*; *Cpt2*; *Acox1*; *Acot2*; *Acaa2*	13.636	10.423–28.083	10	1

Category Name	No. of Active Genes/ Platform Genes in Gene Set	% Gene Set Coverage	Active Genes	BMD_{1Std} Median of Gene Set Transcripts (mg/kg)	Median BMD_{L1Std}–BMD_{U1Std} (mg/kg)	Genes with Changed Direction Up	Genes with Changed Direction Down
GO:0044282 small molecule catabolic process	15/120	13%	*Sult1e1*; *Sult1b1*; *Gcdh*; *Ehhadh*; *Eci2*; *Eci1*; *Ech1*; *Decr1*; *Dao*; *Crat*; *Cpt2*; *Acox1*; *Acot4*; *Acot2*; *Acaa2*	13.636	8.410–28.083	14	1
GO:0006635 fatty acid beta-oxidation	10/33	30%	*Gcdh*; *Ehhadh*; *Eci2*; *Eci1*; *Ech1*; *Decr1*; *Crat*; *Cpt2*; *Acox1*; *Acaa2*	13.834	9.416–29.682	9	1
GO:0030258 lipid modification	14/70	20%	*Pparg*; *Gcdh*; *Ephx2*; *Ehhadh*; *Eci2*; *Eci1*; *Ech1*; *Decr1*; *Cyp4a1*; *Cyp2e1*; *Crat*; *Cpt2*; *Acox1*; *Acaa2*	13.834	9.416–29.034	13	1
GO:0017001 antibiotic catabolic process	3/22	14%	*Ugt2b1*; *Sult1e1*; *Sult1b1*	15.463	7.694–35.088	3	0
GO:0006805 xenobiotic metabolic process	9/62	15%	*Ugt2b1*; *Sult1b1*; *Cyp2j4*; *Cyp2e1*; *Cyp2d3*; *Cyp2c24*; *Cyp2c13*; *Cyp2c11*; *Cyp2a1*	15.463	8.238–35.088	9	0
GO:1901361 organic cyclic compound catabolic process	6/89	7%	*Ugt2b1*; *Sult1e1*; *Srd5a1*; *Ephx2*; *Dao*; *Akr7a3*	15.682	9.448–32.741	5	1

BMD_{1Std} = benchmark dose corresponding to a benchmark response set to one standard deviation from the mean; BMD_{L1Std} = benchmark dose lower confidence limit corresponding to a benchmark response set to one standard deviation from the mean; BMD_{U1Std} = benchmark dose upper confidence limit corresponding to a benchmark response set to one standard deviation from the mean; GO = Gene Ontology.

[a]Definitions of GO terms were adapted from the Gene Ontology Resource.[30] Official gene symbols from the Rat Genome Database[31] are shown in the "Active Genes" column.

GO process description version: https://doi.org/10.22427/NTP-DATA-002-00600-0002-000-0.
GO:0045638 negative regulation of myeloid cell differentiation: Any process that stops, prevents, or reduces the frequency, rate, or extent of myeloid cell differentiation.
GO:0001817 regulation of cytokine production: Any process that modulates the frequency, rate, or extent of production of a cytokine.
GO:0007611 learning or memory: The acquisition and processing of information and/or the storage and retrieval of this information over time.
GO:0030178 negative regulation of Wnt signaling pathway: Any process that stops, prevents, or reduces the frequency, rate, or extent of the Wnt signaling pathway.
GO:0007612 learning: Any process in an organism in which a relatively long-lasting adaptive behavioral change occurs as the result of experience.
GO:0006695 cholesterol biosynthetic process: The chemical reactions and pathways resulting in the formation of cholesterol, cholest-5-en-3 beta-ol, the principal sterol of vertebrates and the precursor of many steroids, including bile acids and steroid hormones.
GO:0043409 negative regulation of MAPK cascade: Any process that stops, prevents, or reduces the frequency, rate, or extent of signal transduction mediated by the MAPKKK cascade.
GO:0014072 response to isoquinoline alkaloid: Any process that results in a change in state or activity of a cell or an organism (in terms of movement, secretion, enzyme production, gene expression, etc.) as a result of an isoquinoline alkaloid stimulus. An isoquinoline alkaloid is any member of a group of compounds with the heterocyclic ring structure of benzo(c)pyridine which is a structure characteristic of the group of opium alkaloids.
GO:0008203 cholesterol metabolic process: The chemical reactions and pathways involving cholesterol, cholest-5-en-3 beta-ol, the principal sterol of vertebrates and the precursor of many steroids, including bile acids and steroid hormones. It is a component of the plasma membrane lipid bilayer and of plasma lipoproteins and can be found in all animal tissues.
GO:0051412 response to corticosterone: Any process that results in a change in state or activity of a cell or an organism (in terms of movement, secretion, enzyme production, gene expression, etc.) as a result of a corticosterone stimulus. Corticosterone is a 21-carbon steroid hormone of the corticosteroid type, produced in the cortex of the adrenal glands. In many species, corticosterone is the principal glucocorticoid, involved in regulation of fuel metabolism, immune reactions, and stress responses.
GO:0018958 phenol-containing compound metabolic process: The chemical reactions and pathways involving a phenol, any compound containing one or more hydroxyl groups directly attached to an aromatic carbon ring.
GO:0046395 carboxylic acid catabolic process: The chemical reactions and pathways resulting in the breakdown of carboxylic acids, any organic acid containing one or more carboxyl (-COOH) groups.
GO:0044242 cellular lipid catabolic process: The chemical reactions and pathways resulting in the breakdown of lipids, as carried out by individual cells.
GO:0009062 fatty acid catabolic process: The chemical reactions and pathways resulting in the breakdown of a fatty acid, any of the aliphatic monocarboxylic acids that can be liberated by hydrolysis from naturally occurring fats and oils. Fatty acids are predominantly straight-chain acids of 4 to 24 carbon atoms, which may be saturated or unsaturated; branched fatty acids and hydroxy fatty acids also occur, and very long-chain acids of over 30 carbons are found in waxes.
GO:0044282 small molecule catabolic process: The chemical reactions and pathways resulting in the breakdown of small molecules, any low molecular weight, monomeric, nonencoded molecule.
GO:0006635 fatty acid beta-oxidation: A fatty acid oxidation process that results in the complete oxidation of a long-chain fatty acid. Fatty acid beta-oxidation begins with the addition of coenzyme A to a fatty acid and occurs by successive cycles of reactions during each of which the fatty acid is shortened by a two-carbon fragment removed as acetyl-coenzyme A; the cycle continues until only two or three carbons remain (as acetyl-CoA or propionyl-CoA respectively).
GO:0030258 lipid modification: The covalent alteration of one or more fatty acids in a lipid, resulting in a change in the properties of the lipid.
GO:0017001 antibiotic catabolic process: The chemical reactions and pathways resulting in the breakdown of antibiotic, a substance produced by or derived from certain fungi, bacteria, and other organisms that can destroy or inhibit the growth of other microorganisms.
GO:0006805 xenobiotic metabolic process: The chemical reactions and pathways involving a xenobiotic compound; a compound foreign to the organism exposed to it. It may be synthesized by another organism (like ampicillin) or it can be a synthetic chemical.
GO:1901361 organic cyclic compound catabolic process: The chemical reactions and pathways resulting in the breakdown of organic cyclic compound.

Table 10. Top 10 Kidney Gene Ontology Biological Process Gene Sets Ranked by Potency of Perturbation, Sorted by Benchmark Dose Median[a]

Category Name	No. of Active Genes/ Platform Genes in Gene Set	% Gene Set Coverage	Active Genes	BMD_{1std} Median of Gene Set Transcripts (mg/kg)	Median BMD_{L1Std}–BMD_{U1Std} (mg/kg)	Genes with Changed Direction Up	Genes with Changed Direction Down
Male							
GO:0045444 fat cell differentiation	3/34	9%	*Srebf1*; *Pex11a*; *Cebpd*	8.745	5.224–15.487	1	2
GO:0006984 ER-nucleus signaling pathway	3/12	25%	*Srebf1*; *Insig1*; *Bcl2l11*	8.745	5.589–15.487	2	1
GO:0019217 regulation of fatty acid metabolic process	4/45	9%	*Srebf1*; *Ppard*; *Insig1*; *Acadl*	9.340	5.671–17.150	4	0
GO:0050796 regulation of insulin secretion	3/50	6%	*Srebf1*; *Ppard*; *Hadh*	9.934	5.754–18.814	3	0
GO:0051301 cell division	4/79	5%	*Top2a*; *Cenpw*; *Cdca3*; *Cdc20*	10.989	7.802–19.064	4	0
GO:0034329 cell junction assembly	3/41	7%	*Lama3*; *Fgf13*; *Ect2*	11.880	8.320–21.047	2	1
GO:0033157 regulation of intracellular protein transport	6/73	8%	*Srebf1*; *Plk3*; *Kif20b*; *Insig1*; *Ect2*; *C2cd5*	12.192	8.490–21.873	4	2
GO:0002244 hematopoietic progenitor cell differentiation	3/31	10%	*Top2a*; *Herc6*; *Cebpd*	12.299	8.517–22.796	2	1
GO:0007059 chromosome segregation	3/37	8%	*Top2a*; *Cenpw*; *Cenpf*	12.299	8.517–22.796	3	0
GO:0032465 regulation of cytokinesis	3/28	11%	*Plk3*; *Kif20b*; *Ect2*	12.504	8.661–22.699	2	1

Category Name	No. of Active Genes/ Platform Genes in Gene Set	% Gene Set Coverage	Active Genes	BMD_{1std} Median of Gene Set Transcripts (mg/kg)	Median BMD_{L1Std}–BMD_{U1Std} (mg/kg)	Genes with Changed Direction Up	Genes with Changed Direction Down
Female							
GO:0051302 regulation of cell division	3/51	6%	*Kif18b*; *Ect2*; *Aspm*	10.324	7.461–16.862	3	0
GO:0007059 chromosome segregation	3/37	8%	*Top2a*; *Ska1*; *Kif18b*	11.921	8.348–21.048	3	0
GO:0051301 cell division	7/79	9%	*Top2a*; *Ska1*; *Kif18b*; *Cks2*; *Cdca3*; *Ccnd1*; *Aspm*	11.921	8.348–21.048	7	0
GO:0070507 regulation of microtubule cytoskeleton organization	3/53	6%	*Ska1*; *Ckap2*; *Atf5*	12.122	8.470–21.380	2	1
GO:0022402 cell cycle process	10/191	5%	*Top2a*; *Kntc1*; *Kif22*; *Kif18b*; *Ect2*; *Cks2*; *Ckap2*; *Cdkn1a*; *Ccnd1*; *Aspm*	13.539	9.169–26.565	9	1
GO:1903047 mitotic cell cycle process	9/146	6%	*Top2a*; *Kntc1*; *Kif22*; *Kif18b*; *Ect2*; *Cks2*; *Ckap2*; *Cdkn1a*; *Ccnd1*	13.839	9.316–27.695	8	1
GO:1903046 meiotic cell cycle process	3/29	10%	*Top2a*; *Cks2*; *Aspm*	13.839	9.316–27.695	3	0
GO:0048285 organelle fission	3/20	15%	*Top2a*; *Mx2*; *Cks2*	14.420	9.624–29.096	2	1
GO:0033762 response to glucagon	4/18	22%	*Srebf1*; *Pck1*; *Hmgcs2*; *Cry1*	20.917	13.412–40.119	3	1
GO:0032869 cellular response to insulin stimulus	4/62	6%	*Srebf1*; *Pck1*; *Hmgcs2*; *Ccl2*	20.917	14.761–40.119	3	1

BMD_{1Std} = benchmark dose corresponding to a benchmark response set to one standard deviation from the mean; BMD_{L1Std} = benchmark dose lower confidence limit corresponding to a benchmark response set to one standard deviation from the mean; BMD_{U1Std} = benchmark dose upper confidence limit corresponding to a benchmark response set to one standard deviation from the mean; GO = Gene Ontology.

[a]Definitions of GO terms were adapted from the Gene Ontology Resource.[30] Official gene symbols from the Rat Genome Database[31] are shown in the "Active Genes" column.
GO process description version: https://doi.org/10.22427/NTP-DATA-002-00600-0002-000-0.
GO:0045444 fat cell differentiation: The process in which a relatively unspecialized cell acquires specialized features of an adipocyte, an animal connective tissue cell specialized for the synthesis and storage of fat.
GO:0006984 ER-nucleus signaling pathway: Any series of molecular signals that conveys information from the endoplasmic reticulum to the nucleus, usually resulting in a change in transcriptional regulation.
GO:0019217 regulation of fatty acid metabolic process: Any process that modulates the frequency, rate, or extent of the chemical reactions and pathways involving fatty acids.
GO:0050796 regulation of insulin secretion: Any process that modulates the frequency, rate, or extent of the regulated release of insulin.
GO:0051301 cell division: The process resulting in division and partitioning of components of a cell to form more cells; may or may not be accompanied by the physical separation of a cell into distinct, individually membrane-bounded daughter cells.
GO:0034329 cell junction assembly: A cellular process that results in the aggregation, arrangement, and bonding together of a set of components to form a cell junction.
GO:0033157 regulation of intracellular protein transport: Any process that modulates the frequency, rate, or extent of the directed movement of proteins within cells.
GO:0002244 hematopoietic progenitor cell differentiation: The process in which precursor cell type acquires the specialized features of a hematopoietic progenitor cell, a class of cell types including myeloid progenitor cells and lymphoid progenitor cells.
GO:0007059 chromosome segregation: The process in which genetic material, in the form of chromosomes, is organized into specific structures and then physically separated and apportioned to two or more sets. In eukaryotes, chromosome segregation begins with the condensation of chromosomes, includes chromosome separation, and ends when chromosomes have completed movement to the spindle poles.
GO:0032465 regulation of cytokinesis: Any process that modulates the frequency, rate, or extent of the division of the cytoplasm of a cell and its separation into two daughter cells.
GO:0051302 regulation of cell division: Any process that modulates the frequency, rate, or extent of the physical partitioning and separation of a cell into daughter cells.
GO:0070507 regulation of microtubule cytoskeleton organization: Any process that modulates the frequency, rate, or extent of the formation, arrangement of constituent parts, or disassembly of cytoskeletal structures comprising microtubules and their associated proteins.
GO:0022402 cell cycle process: The cellular process that ensures successive accurate and complete genome replication and chromosome segregation.
GO:1903047 mitotic cell cycle process: A process that is part of the mitotic cell cycle.
GO:1903046 meiotic cell cycle process: A process that is part of the meiotic cell cycle.
GO:0048285 organelle fission: The creation of two or more organelles by division of one organelle.
GO:0033762 response to glucagon: Any process that results in a change in state or activity of a cell or an organism (in terms of movement, secretion, enzyme production, gene expression, etc.) as a result of a glucagon stimulus.
GO:0032869 cellular response to insulin stimulus: Any process that results in a change in state or activity of a cell (in terms of movement, secretion, enzyme production, gene expression, etc.) as a result of an insulin stimulus. Insulin is a polypeptide hormone produced by the islets of Langerhans of the pancreas in mammals and by the homologous organs of other organisms.

Gene Benchmark Dose Analysis

The top 10 genes based on BMD potency in the liver and kidney (fold change >|2|, significant Williams trend test, global goodness-of-fit p value >0.1, and $BMD_U/BMD_L \leq 40$) are shown in Table 11 and Table 12. As with the GO analysis, the biological or toxicological significance of the changes in gene expression shown in Table 11 and Table 12 should be interpreted with caution. The data primarily should be considered a metric of potency for chemical-induced transcriptional changes that could serve as a conservative surrogate of estimated biological potency, and by extension toxicological potency, when more definitive toxicological data are unavailable.

No liver genes in male or female rats had estimated BMD median values <0.050 mg/kg. In male rats, the most sensitive upregulated genes with a calculated BMD were *Gsta2* (glutathione S-transferase alpha 2), *Gsta5* (glutathione S-transferase alpha 5), *Crot* (carnitine O-octanoyltransferase), *Slc27a2* (solute carrier family 27 member 2), *Acaa1a* (acetyl-CoA acyltransferase 1A), and *Acaa1b* (acetyl-Coenzyme A acyltransferase 1B) with BMDs (BMD_Ls)

of 5.725 (1.686), 5.725 (1.686), 7.423 (5.757), 7.622 (5.499), 8.417 (7.129), and 8.417 (7.129) mg/kg, respectively. The most sensitive genes exhibiting a decrease in expression were *Egr1* (early growth response 1), *Zfp354a* (zinc finger protein 354A), *Tsku* (tsukushi, small leucine rich proteoglycan), and *Cyp7a1* (cytochrome P450 family 7 subfamily A member 1) with BMDs (BMD_{LS}) of 0.750 (0.186), 0.835 (0.271), 1.384 (0.541), and 5.721 (0.985) mg/kg, respectively.

In female rats, the most sensitive upregulated liver genes with a calculated BMD were *Dao* (D-amino-acid oxidase), *Ephx2* (epoxide hydrolase 2), *Ehhadh* (enoyl-CoA hydratase and 3-hydroxyacyl CoA dehydrogenase), *Cyp2b1* (cytochrome P450, family 2, subfamily b, polypeptide 1), *Loc108348266*/*Cyp2b1* (cytochrome P450 2B1), *Cyp2c6v1* (cytochrome P450, family 2, subfamily C, polypeptide 6, variant 1), *Loc100911718* (cytochrome P450 2C6-like), and *Ech1* (enoyl-CoA hydratase 1) with BMDs (BMD_{LS}) of 6.134 (2.436), 6.441 (2.664), 7.300 (5.266), 7.456 (5.106), 7.456 (5.106), 9.829 (7.252), 9.829 (7.252), and 9.874 (6.591) mg/kg, respectively. The most sensitive genes exhibiting a decrease in expression were *A2m* (alpha-2-macroglobulin) and *Loc100911545*/*A2m* (alpha-2-macroglobulin), both with a BMD (BMD_{L}) of 1.163 (0.179) mg/kg.

None of the top 10 most sensitive kidney genes in male or female rats had estimated BMD median values <0.050 mg/kg. In male rats, the most sensitive upregulated genes with a calculated BMD were *Insig1* (insulin induced gene 1), *Srebf1* (sterol regulatory element-binding transcription factor 1), *Fads1* (fatty acid desaturase 1), *Ppard* (peroxisome proliferator-activated receptor delta), *Decr1* (2,4-dienoyl-CoA reductase 1), *Acot2* (acyl-CoA thioesterase 2), *Acaa1a* (acetyl-CoA acyltransferase 1A), *Acaa1b* (acetyl-Coenzyme A acyltransferase 1B), and *Fasn* (fatty acid synthase) with BMDs (BMD_{LS}) of 7.612 (5.589), 8.745 (5.224), 9.357 (6.123), 9.934 (5.754), 12.862 (10.721), 13.201 (10.994), 13.398 (11.228), 13.398 (11.228), and 13.486 (11.223) mg/kg, respectively. One gene, *Loc100911814*/*Spink1l* (glycine decarboxylase), was downregulated with a BMD (BMD_{L}) of 0.510 (0.212) mg/kg.

In female rats, the most sensitive upregulated kidney genes with a calculated BMD were *Cdca3* (cell division cycle associated 3), *Pck1* (phosphoenolpyruvate carboxykinase 1), *Ube2t* (ubiquitin-conjugating enzyme E2T), *Srebf1* (sterol regulatory element-binding transcription factor 1), *Ckap2* (cytoskeleton associated protein 2), *Lilra3* (leukocyte immunoglobulin-like receptor, subfamily A (without TM domain), member 3), *Lilrb3l* (leukocyte immunoglobulin-like receptor, subfamily B (with TM and ITIM domains), member 3-like), and *Acaa1a* (acetyl-CoA acyltransferase 1A) with BMDs (BMD_{LS}) of 2.619 (0.978), 5.515 (1.341), 10.991 (7.866), 11.236 (4.944), 12.122 (8.470), 17.020 (10.650), 17.020 (10.650), and 17.682 (14.617) mg/kg, respectively. The most sensitive genes exhibiting a decrease in expression were *Slc10a1* (solute carrier family 10 member 1) and *Cyp2c24* (cytochrome P450, family 2, subfamily c, polypeptide 24) with BMDs (BMD_{LS}) of 7.968 (6.075) and 10.565 (7.636) mg/kg, respectively.

Table 11. Top 10 Liver Genes Ranked by Potency of Perturbation, Sorted by Benchmark Dose Median[a]

Gene Symbol	Entrez Gene IDs	Probe IDs[b]	BMD_{1Std} (BMD_{L1std}–BMD_{U1std}) in mg/kg	Maximum Fold Change	Direction of Expression Change
Male					
Egr1	24330	EGR1_8533	0.750 (0.186–4.702)	4.2	DOWN
Zfp354a	24522	ZFP354A_10203	0.835 (0.271–2.999)	4.6	DOWN
Tsku	308843	TSKU_10094	1.384 (0.541–4.109)	3.0	DOWN
Cyp7a1	25428	CYP7A1_8430	5.721 (0.985–22.363)	4.6	DOWN
Gsta2	24422	GSTA2_8756	5.725 (1.686–19.439)	2.3	UP
Gsta5	494499	GSTA2_8756	5.725 (1.686–19.439)	2.3	UP
Crot	83842	CROT_8384	7.423 (5.757–10.316)	6.0	UP
Slc27a2	65192	SLC27A2_9860	7.622 (5.499–13.393)	2.2	UP
Acaa1a	24157	ACAA1A_7954	8.417 (7.129–10.157)	13.3	UP
Acaa1b	501072	ACAA1A_7954	8.417 (7.129–10.157)	13.3	UP
Female					
A2m	24153	A2M_7932	1.163 (0.179–7.061)	2.3	DOWN
Loc100911545/A2m	100911545	A2M_7932	1.163 (0.179–7.061)	2.3	DOWN
Dao	114027	DAO_8437	6.134 (2.436–16.203)	2.1	UP
Ephx2	65030	EPHX2_33282	6.441 (2.664–17.347)	2.4	UP
Ehhadh	171142	EHHADH_8534	7.300 (5.266–11.878)	4.0	UP
Cyp2b1	24300	CYP2B1_32451	7.456 (5.106–13.104)	31.5	UP
Loc108348266/Cyp2b1	108348266	CYP2B1_32451	7.456 (5.106–13.104)	31.5	UP
Cyp2c6v1	293989	CYP2C6V1_33169	9.829 (7.252–14.982)	2.4	UP
Loc100911718	100911718	CYP2C6V1_33169	9.829 (7.252–14.982)	2.4	UP
Ech1	64526	ECH1_8516	9.874 (6.591–19.440)	3.6	UP

BMD_{1Std} = benchmark dose corresponding to a benchmark response set to one standard deviation from the mean; BMD_{L1Std} = benchmark dose lower confidence limit corresponding to a benchmark response set to one standard deviation from the mean; BMD_{U1Std} = benchmark dose upper confidence limit corresponding to a benchmark response set to one standard deviation from the mean.

[a]Descriptions of orthologous human genes are shown due to the increased detail available in public resources such as UniprotKB[32] and Entrez Gene.[33] Gene definitions adapted from Human UniprotKB were used as the primary resource due to the greater breadth of annotation and depth of functional detail provided. Gene definitions adapted from Rat UniprotKB were used as the secondary resource if the primary source did not provide a detailed description of function. Human Entrez Gene was used as the third resource. Rat Entrez Gene was used as the fourth resource.

[b]In some cases, a probe may map to more than one gene, resulting in duplicate reporting of that probe mapped to different genes.

Gene definition version: https://doi.org/10.22427/NTP-DATA-002-00600-0002-000-0.

***Egr1*:** Human Uniprot function (Human *EGR1*): Transcriptional regulator (PubMed20121949). Recognizes and binds to the DNA sequence 5'-GCG(T/G)GGGCG-3'(EGR-site) in the promoter region of target genes (by similarity). Binds double-stranded target DNA, irrespective of the cytosine methylation status (PubMed25258363, PubMed25999311). Regulates the transcription of numerous target genes, and thereby plays an important role in regulating the response to growth factors, DNA damage, and ischemia. Plays a role in the regulation of cell survival, proliferation, and cell death. Activates expression of p53/TP53 and TGFB1, and thereby helps prevent tumor formation. Required for normal progress through mitosis and normal proliferation of hepatocytes after partial hepatectomy. Mediates responses to ischemia and hypoxia; regulates the expression of proteins such as IL1B and CXCL2 that are involved in inflammatory processes and development of tissue damage after ischemia. Regulates

biosynthesis of luteinizing hormone (LHB) in the pituitary (by similarity). Regulates the amplitude of the expression rhythms of clock genes ARNTL/BMAL1, PER2 and NR1D1 in the liver via the activation of PER1 (clock repressor) transcription. Regulates the rhythmic expression of core-clock gene ARNTL/BMAL1 in the suprachiasmatic nucleus (SCN) (by similarity). {ECO0000250|UniProtKBP08046, ECO0000269|PubMed20121949, ECO0000269|PubMed25258363, ECO0000269|PubMed25999311}.

***Zfp354a*:** Rat Uniprot Function (Human *ZNF354A*): It may play a role in renal development and may also be involved in the repair of the kidney after ischemia-reperfusion or folic acid administration.

***Tsku*:** Human Uniprot function (Human *TSKU*): Contributes to various developmental events and other processes such as wound healing and cholesterol homeostasis through its interactions with multiple signaling pathways. Wnt signaling inhibitor which competes with WNT2B for binding to Wnt receptor FZD4 and represses WNT2B-dependent development of the peripheral eye. Plays a role in regulating the hair cycle by controlling TGFB1 signaling. Required for the development of the anterior commissure in the brain by inhibiting neurite outgrowth. Essential for terminal differentiation of hippocampal neural stem cells. Plays a role in regulating bone elongation and bone mass by modulating growth plate chondrocyte function and overall body size. Required for development of the inner ear through its involvement in stereocilia formation in inner hair cells. Facilitates wound healing by inhibiting secretion of TGFB1 from macrophages which prevents myofibroblast differentiation, maintaining inflammatory cell quiescence. Plays a role in cholesterol homeostasis by reducing circulating high-density lipoprotein cholesterol, lowering cholesterol efflux capacity and decreasing cholesterol-to-bile acid conversion in the liver. In one study, shown to negatively regulate sympathetic innervation in brown fat, leading to reduced energy expenditure. In another study, shown not to affect brown fat thermogenic capacity, body weight gain or glucose homeostasis.

***Cyp7a1*:** Human Uniprot function (Human *CYP7A1*): A cytochrome P450 monooxygenase involved in the metabolism of endogenous cholesterol and its oxygenated derivatives (oxysterols) (PubMed11013305, PubMed12077124, PubMed19965590, PubMed2384150, PubMed21813643). Mechanistically, uses molecular oxygen inserting one oxygen atom into a substrate, and reducing the second into a water molecule, with two electrons provided by NADPH via cytochrome P450 reductase (CPR; NADPH-ferrihemoprotein reductase) (PubMed2384150, PubMed11013305, PubMed12077124, PubMed19965590, PubMed21813643). Functions as a critical regulatory enzyme of bile acid biosynthesis and cholesterol homeostasis. Catalyzes the hydroxylation of carbon-hydrogen bond at 7-alpha position of cholesterol, a rate-limiting step in cholesterol catabolism and bile acid biosynthesis (PubMed12077124, PubMed19965590, PubMed2384150). 7-alpha hydroxylates several oxysterols, including 4beta-hydroxycholesterol and 24-hydroxycholesterol (PubMed11013305, PubMed12077124). Catalyzes the oxidation of the 7,8 double bond of 7-dehydrocholesterol and lathosterol with direct and predominant formation of the 7-keto derivatives (PubMed21813643). {ECO0000269|PubMed11013305, ECO0000269|PubMed12077124, ECO0000269|PubMed19965590, ECO0000269|PubMed21813643, ECO0000269|PubMed2384150}.

***Gsta2*:** Human Uniprot function (Human *GSTA2*): Conjugation of reduced glutathione to a wide number of exogenous and endogenous hydrophobic electrophiles.

***Gsta5*:** Rat Uniprot Function (Human *GSTA5*): Conjugation of reduced glutathione to a wide number of exogenous and endogenous hydrophobic electrophiles. Has substantial activity toward aflatoxin B1-8,9-epoxide.

***Crot*:** Human Uniprot function (Human *CROT*): Beta-oxidation of fatty acids. The highest activity concerns the C6 to C10 chain length substrate. Converts the end product of pristanic acid beta-oxidation, 4,8-dimethylnonanoyl-CoA, to its corresponding carnitine ester. {ECO0000269|PubMed10486279}.

***Slc27a2*:** Human Uniprot function (Human *SLC27A2*): Acyl-CoA synthetase that activates long-chain and very long-chain fatty acids (VLCFAs) by catalyzing the formation of fatty acyl-CoA (PubMed10198260, PubMed10749848, PubMed11980911). Can also activate branched-chain fatty acids such as phytanic acid and pristanic acid (PubMed10198260). Does not activate C24 bile acids, cholate and chenodeoxycholate (PubMed11980911). In vitro, activates 3-alpha,7-alpha,12-alpha-trihydroxy-5-beta-cholestanate (THCA), the C27 precursor of cholic acid deriving from the de novo synthesis from cholesterol (PubMed11980911). Exhibits long-chain fatty acids (LCFA) transport activity and plays an important role in hepatic fatty acid uptake (PubMed20530735). {ECO0000269|PubMed10198260, ECO0000269|PubMed10749848, ECO0000269|PubMed11980911, ECO0000269|PubMed20530735}. FUNCTION [Isoform 1] Exhibits both long-chain fatty acids (LCFA) transport activity and acyl-CoA synthetase toward very long-chain fatty acids (PubMed21768100). Shows a preference for generating CoA derivatives of n-3 fatty acids, which are preferentially trafficked into phosphatidylinositol (PubMed21768100). {ECO0000269|PubMed21768100}. FUNCTION [Isoform 2] Exhibits long-chain fatty acids (LCFA) transport activity but lacks acyl-CoA synthetase toward very long-chain fatty acids. {ECO0000269|PubMed21768100}.

***Acaa1a*:** Human Entrez Gene Summary (Human *ACAA1*): This gene encodes an enzyme operative in the beta-oxidation system of the peroxisomes. Deficiency of this enzyme leads to pseudo-Zellweger syndrome. Alternative splicing results in multiple transcript variants. [provided by RefSeq, Jul 2008]

***Acaa1b*:** Human Entrez Gene Summary (Human *ACAA1*): This gene encodes an enzyme operative in the beta-oxidation system of the peroxisomes. Deficiency of this enzyme leads to pseudo-Zellweger syndrome. Alternative splicing results in multiple transcript variants. [provided by RefSeq, Jul 2008]

***A2m*:** Human Uniprot function (Human *A2M*): Is able to inhibit all four classes of proteinases by a unique ‘trapping’ mechanism. This protein has a peptide stretch, called the ‘bait region’ which contains specific cleavage sites for different proteinases. When a proteinase cleaves the bait region, a conformational change is induced in the protein which traps the proteinase. The entrapped enzyme remains active against low molecular weight substrates (activity against high molecular weight substrates is greatly reduced). Following cleavage in the bait region, a thioester bond is hydrolyzed and mediates the covalent binding of the protein to the proteinase.

***LOC100911545*/*A2m*:** Human Uniprot function (Human *A2M*): Is able to inhibit all four classes of proteinases by a unique 'trapping' mechanism. This protein has a peptide stretch, called the 'bait region' which contains specific cleavage sites for different proteinases. When a proteinase cleaves the bait region, a conformational change is induced in the protein which traps the proteinase. The entrapped enzyme remains active against low molecular weight substrates (activity against high molecular weight substrates is greatly reduced). Following cleavage in the bait region, a thioester bond is hydrolyzed and mediates the covalent binding of the protein to the proteinase.
***Dao*:** Human Uniprot function (Human *DAO*): Regulates the level of the neuromodulator D-serine in the brain. Has high activity toward D-DOPA and contributes to dopamine synthesis. Could act as a detoxifying agent which removes D-amino acids accumulated during aging. Acts on a variety of D-amino acids with a preference for those having small hydrophobic side chains followed by those bearing polar, aromatic, and basic groups. Does not act on acidic amino acids. {ECO0000269|PubMed17303072}.
***Ephx2*:** Human Uniprot function (Human *EPHX2*): Bifunctional enzyme (PubMed12574510). The C-terminal domain has epoxide hydrolase activity and acts on epoxides (alkene oxides, oxiranes) and arene oxides (PubMed12869654, PubMed12574510, PubMed22798687). Plays a role in xenobiotic metabolism by degrading potentially toxic epoxides (by similarity). Also determines steady-state levels of physiological mediators (PubMed12869654, PubMed12574510, PubMed22798687, PubMed21217101). {ECO0000250|UniProtKBP80299, ECO0000269|PubMed12574508, ECO0000269|PubMed12574510, ECO0000269|PubMed12869654, ECO0000269|PubMed21217101, ECO0000269|PubMed22798687}. FUNCTION Bifunctional enzyme (PubMed12574510). The N-terminal domain has lipid phosphatase activity, with the highest activity toward threo-9,10-phosphonooxy-hydroxy-octadecanoic acid, followed by erythro-9,10-phosphonooxy-hydroxy-octadecanoic acid, 12-phosphonooxy-octadec-9Z-enoic acid and 12-phosphonooxy-octadec-9E-enoic acid (PubMed12574510). Has phosphatase activity toward lyso-glycerophospholipids with also some lower activity toward lysolipids of sphingolipid and isoprenoid phosphates (PubMed22217705, PubMed22387545). {ECO0000269|PubMed12574510, ECO0000269|PubMed22217705, ECO0000269|PubMed22387545}.
***Ehhadh*:** Human Uniprot function (Human *EHHADH*): Peroxisomal trifunctional enzyme possessing 2-enoyl-CoA hydratase, 3-hydroxyacyl-CoA dehydrogenase, and delta 3, delta 2-enoyl-CoA isomerase activities. Catalyzes two of the four reactions of the long straight-chain fatty acids peroxisomal beta-oxidation pathway. Optimal isomerase for 2,5 double bonds into 3,5 form isomerization in a range of enoyl-CoA species (probable). Also able to isomerize both 3-*cis* and 3-*trans* double bonds into the 2-*trans* form in a range of enoyl-CoA species (by similarity). With HSD17B4, catalyzes the hydration of trans-2-enoyl-CoA and the dehydrogenation of 3-hydroxyacyl-CoA, but with opposite chiral specificity (PubMed15060085). Regulates the amount of medium-chain dicarboxylic fatty acids which are essential regulators of all fatty acid oxidation pathways (by similarity). Also involved in the degradation of long-chain dicarboxylic acids through peroxisomal beta-oxidation (PubMed15060085). {ECO0000250|UniProtKBP07896, ECO0000250|UniProtKBQ9DBM2, ECO0000269|PubMed15060085, ECO0000305|PubMed15060085}.
***Cyp2b1*:** Human Uniprot function (Human *CYP2B6*): A cytochrome P450 monooxygenase involved in the metabolism of endocannabinoids and steroids (PubMed21289075, PubMed12865317). Mechanistically, uses molecular oxygen inserting one oxygen atom into a substrate, and reducing the second into a water molecule, with two electrons provided by NADPH via cytochrome P450 reductase (NADPH--hemoprotein reductase). Catalyzes the epoxidation of double bonds of arachidonoylethanolamide (anandamide) to 8,9-, 11,12-, and 14,15-epoxyeicosatrienoic acid ethanolamides (EpETrE-Eas), potentially modulating endocannabinoid system signaling (PubMed21289075). Hydroxylates steroid hormones, including testosterone at C-16 and estrogens at C-2 (PubMed21289075, PubMed12865317). Plays a role in the oxidative metabolism of xenobiotics, including plant lipids and drugs (PubMed11695850, PubMed22909231). Acts as a 1,4-cineole 2-exo-monooxygenase (PubMed11695850). {ECO0000269|PubMed11695850, ECO0000269|PubMed12865317, ECO0000269|PubMed21289075, ECO0000269|PubMed22909231}. FUNCTION Allele 2B6*9 Has low affinity for anandamide and can only produce 11,12 EpETrE-Eas. {ECO0000269|PubMed21289075}.
***LOC108348266*/*Cyp2b1*:** Human Uniprot function (Human *CYP2B6*): A cytochrome P450 monooxygenase involved in the metabolism of endocannabinoids and steroids (PubMed21289075, PubMed12865317). Mechanistically, uses molecular oxygen inserting one oxygen atom into a substrate, and reducing the second into a water molecule, with two electrons provided by NADPH via cytochrome P450 reductase (NADPH--hemoprotein reductase). Catalyzes the epoxidation of double bonds of arachidonoylethanolamide (anandamide) to 8,9-, 11,12-, and 14,15-epoxyeicosatrienoic acid ethanolamides (EpETrE-Eas), potentially modulating endocannabinoid system signaling (PubMed21289075). Hydroxylates steroid hormones, including testosterone at C-16 and estrogens at C-2 (PubMed21289075, PubMed12865317). Plays a role in the oxidative metabolism of xenobiotics, including plant lipids and drugs (PubMed11695850, PubMed22909231). Acts as a 1,4-cineole 2-exo-monooxygenase (PubMed11695850).
***Cyp2c6v1*:** Human Uniprot function (Human *CYP2C19*): A cytochrome P450 monooxygenase involved in the metabolism of polyunsaturated fatty acids (PUFA) (PubMed18577768, PubMed19965576, PubMed20972997). Mechanistically, uses molecular oxygen inserting one oxygen atom into a substrate, and reducing the second into a water molecule, with two electrons provided by NADPH via cytochrome P450 reductase (NADPH--hemoprotein reductase) (PubMed18577768, PubMed19965576, PubMed20972997). Catalyzes the hydroxylation of carbon-hydrogen bonds. Hydroxylates PUFA specifically at the omega-1 position (PubMed18577768). Catalyzes the epoxidation of double bonds of PUFA (PubMed20972997, PubMed19965576). Also metabolizes plant monoterpenes such as limonene. Oxygenates (R)- and (S)-limonene to produce carveol and perillyl alcohol (PubMed11950794). Responsible for the metabolism of a number of therapeutic agents such as the anticonvulsant drug S-mephenytoin, omeprazole, proguanil, certain barbiturates, diazepam, propranolol, citalopram, and imipramine. Hydroxylates

fenbendazole at the 4' position (PubMed23959307). {ECO0000269|PubMed11950794, ECO0000269|PubMed18577768, ECO0000269|PubMed19965576, ECO0000269|PubMed20972997, ECO0000269|PubMed23959307}.
***LOC100911718*:** Human Uniprot function (Human *CYP2C18*): A cytochrome P450 monooxygenase involved in retinoid metabolism. Hydroxylates all *trans*-retinoic acid (atRA) to 4-hydroxyretinoate and may modulate atRA signaling and clearance. Mechanistically, uses molecular oxygen inserting one oxygen atom into a substrate, and reducing the second into a water molecule, with two electrons provided by NADPH via cytochrome P450 reductase (CPR; NADPH-ferrihemoprotein reductase). CP2CI_HUMAN,P33260
***Ech1*:** Human Uniprot function (Human *ECH1*): Isomerization of 3-*trans*,5-*cis*-dienoyl-CoA to 2-*trans*,4-*trans*-dienoyl-CoA. {ECO0000250|UniProtKBQ62651}.

Table 12. Top 10 Kidney Genes Ranked by Potency of Perturbation, Sorted by Benchmark Dose Median[a]

Gene Symbol	Entrez Gene IDs	Probe IDs[b]	BMD_{1Std} (BMD_{L1std}–BMD_{U1std}) in mg/kg	Maximum Fold Change	Direction of Expression Change
Male					
Loc100911814*/*Spink1l	100911814	LOC100911814_9091	0.510 (0.212–1.639)	3.0	DOWN
Insig1	64194	INSIG1_8906	7.612 (5.589–12.856)	3.8	UP
Srebf1	78968	SREBF1_32750	8.745 (5.224–15.487)	3.8	UP
Fads1	84575	FADS1_8593	9.357 (6.123–15.758)	2.4	UP
Ppard	25682	PPARD_9536	9.934 (5.754–18.814)	2.4	UP
Decr1	117543	DECR1_8458	12.862 (10.721–15.913)	2.2	UP
Acot2	192272	ACOT2_7969	13.201 (10.994–16.357)	2.3	UP
Acaa1a	24157	ACAA1A_7954	13.398 (11.228–16.447)	3.9	UP
Acaa1b	501072	ACAA1A_7954	13.398 (11.228–16.447)	3.9	UP
Fasn	50671	FASN_8611	13.486 (11.223–16.732)	2.3	UP
Female					
Cdca3	297594	CDCA3_8260	2.619 (0.978–7.970)	2.3	UP
Pck1	362282	PCK1_9439	5.515 (1.341–39.672)	2.3	UP
Slc10a1	24777	SLC10A1_9832	7.968 (6.075–11.486)	2.5	DOWN
Cyp2c24	499353	CYP2C24_32875	10.565 (7.636–17.047)	2.3	DOWN
Ube2t	360847	UBE2T_10125	10.991 (7.866–18.206)	2.4	UP
Srebf1	78968	SREBF1_32750	11.236 (4.944–24.577)	2.9	UP
Ckap2	306575	CKAP2_8324	12.122 (8.470–21.380)	2.2	UP
Lilra3	100912499	LILRA3_32676	17.020 (10.650–96.524)	2.5	UP
Lilrb3l	361493	LILRA3_32676	17.020 (10.650–96.524)	2.5	UP
Acaa1a	24157	ACAA1A_7954	17.682 (14.617–22.195)	2.2	UP

BMD_{1Std} = benchmark dose corresponding to a benchmark response set to one standard deviation from the mean; BMD_{L1Std} = benchmark dose lower confidence limit corresponding to a benchmark response set to one standard deviation from the mean; BMD_{U1Std} = benchmark dose upper confidence limit corresponding to a benchmark response set to one standard deviation from the mean.
[a]Descriptions of orthologous human genes are shown due to the increased detail available in public resources such as UniprotKB[32] and Entrez Gene.[33] Gene definitions adapted from Human UniprotKB were used as the primary resource due to the greater breadth of annotation and depth of functional detail provided. Gene definitions adapted from Rat UniprotKB were used as

the secondary resource if the primary source did not provide a detailed description of function. Human Entrez Gene was used as the third resource. Rat Entrez Gene was used as the fourth resource.
[b]In some cases, a probe may map to more than one gene, resulting in duplicate reporting of that probe mapped to different genes.
Gene definition version: https://doi.org/10.22427/NTP-DATA-002-00600-0002-000-0.
***LOC100911814*/*Spink1*:** Human Uniprot function (Human *GLDC*): The glycine cleavage system catalyzes the degradation of glycine. The P protein (GLDC) binds the alpha-amino group of glycine through its pyridoxal phosphate cofactor; CO(2) is released, and the remaining methylamine moiety is then transferred to the lipoamide cofactor of the H protein (GCSH).
***Insig1*:** Human Uniprot function (Human *INSIG1*): Oxysterol-binding protein that mediates feedback control of cholesterol synthesis by controlling both endoplasmic reticulum to Golgi transport of SCAP and degradation of HMGCR (PubMed12202038, PubMed12535518, PubMed16168377, PubMed16399501, PubMed16606821, PubMed32322062). Acts as a negative regulator of cholesterol biosynthesis by mediating the retention of the SCAP-SREBP complex in the endoplasmic reticulum, thereby blocking the processing of sterol regulatory element-binding proteins (SREBPs) SREBF1/SREBP1 and SREBF2/SREBP2 (PubMed12202038, PubMed16399501, PubMed32322062). Binds oxysterol, including 25-hydroxycholesterol, regulating interaction with SCAP and retention of the SCAP-SREBP complex in the endoplasmic reticulum (PubMed32322062). In the presence of oxysterol, it interacts with SCAP, retaining the SCAP-SREBP complex in the endoplasmic reticulum, thereby preventing SCAP from escorting SREBF1/SREBP1 and SREBF2/SREBP2 to the Golgi (PubMed15899885, PubMed32322062). Sterol deprivation or phosphorylation by PCK1 reduce oxysterol-binding, disrupting the interaction between INSIG1 and SCAP, thereby promoting Golgi transport of the SCAP-SREBP complex, followed by processing and nuclear translocation of SREBF1/SREBP1 and SREBF2/SREBP2 (PubMed32322062). Also regulates cholesterol synthesis by regulating degradation of HMGCR initiates the sterol-mediated ubiquitin-mediated endoplasmic reticulum-associated degradation (ERAD) of HMGCR via recruitment of the reductase to the ubiquitin ligases AMFR/gp78 and/or RNF139 (PubMed12535518, PubMed16168377, PubMed22143767). Also regulates degradation of SOAT2/ACAT2 when the lipid levels are low; initiates the ubiquitin-mediated degradation of SOAT2/ACAT2 via recruitment of the ubiquitin ligases AMFR/gp78 (PubMed28604676). {ECO0000269|PubMed12202038, ECO0000269|PubMed12535518, ECO0000269|PubMed15899885, ECO0000269|PubMed16168377, ECO0000269|PubMed16399501, ECO0000269|PubMed16606821, ECO0000269|PubMed22143767, ECO0000269|PubMed28604676, ECO0000269|PubMed32322062}.
***Srebf1*:** Human Uniprot function (Human *SREBF1*): [Sterol regulatory element-binding protein 1] Precursor of the transcription factor form (Processed sterol regulatory element-binding protein 1), which is embedded in the endoplasmic reticulum membrane (PubMed32322062). Low sterol concentrations promote processing of this form, releasing the transcription factor form that translocates into the nucleus and activates transcription of genes involved in cholesterol biosynthesis and lipid homeostasis (by similarity). {ECO0000250|UniProtKBQ9WTN3, ECO0000269|PubMed32322062}. FUNCTION [Processed sterol regulatory element-binding protein 1] Key transcription factor that regulates expression of genes involved in cholesterol biosynthesis and lipid homeostasis (PubMed8402897, PubMed12177166, PubMed32322062). Binds to the sterol regulatory element 1 (SRE-1) (5'-ATCACCCCAC-3'). Has dual sequence specificity binding to both an E-box motif (5'-ATCACGTGA-3') and to SRE-1 (5'-ATCACCCCAC-3') (PubMed8402897, PubMed12177166). Regulates the promoters of genes involved in cholesterol biosynthesis and the LDL receptor (LDLR) pathway of sterol regulation (PubMed8402897, PubMed12177166, PubMed32322062). {ECO0000269|PubMed12177166, ECO0000269|PubMed32322062, ECO0000269|PubMed8402897}. FUNCTION [Isoform SREBP-1A] Isoform expressed only in select tissues, which has higher transcriptional activity compared to SREBP-1C (by similarity). Able to stimulate both lipogenic and cholesterogenic gene expression (PubMed12177166). Has a role in the nutritional regulation of fatty acids and triglycerides in lipogenic organs such as the liver (by similarity). Required for innate immune response in macrophages by regulating lipid metabolism (by similarity). {ECO0000250|UniProtKBQ9WTN3, ECO0000269|PubMed12177166}. FUNCTION [Isoform SREBP-1C] Predominant isoform expressed in most tissues, which has weaker transcriptional activity compared to isoform SREBP-1A (by similarity). Primarily controls expression of lipogenic gene (PubMed12177166). Strongly activates global lipid synthesis in rapidly growing cells (by similarity). {ECO0000250|UniProtKBQ9WTN3, ECO0000269|PubMed12177166}. FUNCTION [Isoform SREBP-1aDelta] The absence of Golgi proteolytic processing requirement makes this isoform constitutively active in transactivation of lipogenic gene promoters. {ECO0000305|PubMed7759101}. FUNCTION [Isoform SREBP-1cDelta] The absence of Golgi proteolytic processing requirement makes this isoform constitutively active in transactivation of lipogenic gene promoters. {ECO0000305|PubMed7759101}.
***Fads1*:** Human Uniprot function (Human *FADS1*): [Isoform 1] Acts as a front-end fatty acyl-coenzyme A (CoA) desaturase that introduces a cis double bond at carbon 5 located between a preexisting double bond and the carboxyl end of the fatty acyl chain. Involved in biosynthesis of highly unsaturated fatty acids (HUFA) from the essential polyunsaturated fatty acids (PUFA) linoleic acid (LA) (182n-6) and alpha-linolenic acid (ALA) (183n-3) precursors. Specifically, desaturates dihomo-gamma-linoleoate (DGLA) (203n-6) and eicosatetraenoate (ETA) (204n-3) to generate arachidonate (AA) (204n-6) and eicosapentaenoate (EPA) (205n-3), respectively (PubMed10601301, PubMed10769175). As a rate-limiting enzyme for DGLA (203n-6) and AA (204n-6)-derived eicosanoid biosynthesis, controls the metabolism of inflammatory lipids like prostaglandin E2, critical for efficient acute inflammatory response and maintenance of epithelium homeostasis. Contributes to membrane phospholipid biosynthesis by providing AA (204n-6) as a major acyl chain esterified into phospholipids. In particular, regulates phosphatidylinositol-4,5-bisphosphate levels, modulating inflammatory cytokine production in T-cells (by similarity). Also desaturates (11E)-octadecenoate (trans-vaccenoate)(181n-9), a metabolite in the biohydrogenation pathway of LA (182n-6) (by similarity). {ECO0000250|UniProtKBQ920L1, ECO0000250|UniProtKBQ920R3, ECO0000269|PubMed10601301,

ECO0000269|PubMed10769175}. FUNCTION [Isoform 2] Does not exhibit any catalytic activity toward 203n-6, but it may enhance FADS2 activity. {ECO0000250|UniProtKBA4UVI1}.
***Ppard*:** Human Uniprot function (Human *PPARD*): Ligand-activated transcription factor. Receptor that binds peroxisome proliferators such as hypolipidemic drugs and fatty acids. Has a preference for polyunsaturated fatty acids, such as gamma-linoleic acid and eicosapentanoic acid. Once activated by a ligand, the receptor binds to promoter elements of target genes. Regulates the peroxisomal beta-oxidation pathway of fatty acids. Functions as transcription activator for the acyl-CoA oxidase gene. Decreases expression of NPC1L1 once activated by a ligand. {ECO0000269|PubMed1333051, ECO0000269|PubMed15604518}.
***Decr1*:** Human Uniprot function (Human *DECR1*): Auxiliary enzyme of beta-oxidation. It participates in the metabolism of unsaturated fatty enoyl-CoA esters having double bonds in both even- and odd-numbered positions in mitochondria. Catalyzes the NADP-dependent reduction of 2,4-dienoyl-CoA to yield trans-3-enoyl-CoA. {ECO0000269|PubMed15531764}.
***Acot2*:** Human Uniprot function (Human *ACOT2*): Acyl-CoA thioesterases are a group of enzymes that catalyze the hydrolysis of acyl-CoAs to the free fatty acid and coenzyme A (CoASH), providing the potential to regulate intracellular levels of acyl-CoAs, free fatty acids and CoASH (PubMed16940157). Acyl-coenzyme A thioesterase 2/ACOT2 displays higher activity toward long-chain acyl-CoAs (C14-C20) (PubMed16940157, PubMed10944470). The enzyme is involved in enhancing the hepatic fatty acid oxidation in mitochondria (by similarity). {ECO0000250|UniProtKBQ9QYR9, ECO0000269|PubMed10944470, ECO0000269|PubMed16940157, ECO0000303|PubMed16940157}.
***Acaa1a*:** Human Entrez Gene Summary (Human *ACAA1*): This gene encodes an enzyme operative in the beta-oxidation system of the peroxisomes. Deficiency of this enzyme leads to pseudo-Zellweger syndrome. Alternative splicing results in multiple transcript variants. [provided by RefSeq, Jul 2008]
***Acaa1b*:** Human Entrez Gene Summary (Human *ACAA1*): This gene encodes an enzyme operative in the beta-oxidation system of the peroxisomes. Deficiency of this enzyme leads to pseudo-Zellweger syndrome. Alternative splicing results in multiple transcript variants. [provided by RefSeq, Jul 2008]
***Fasn*:** Human Uniprot function (Human *FASN*): Fatty acid synthetase is a multifunctional enzyme that catalyzes the de novo biosynthesis of long-chain saturated fatty acids starting from acetyl-CoA and malonyl-CoA in the presence of NADPH. This multifunctional protein contains seven catalytic activities and a site for the binding of the prosthetic group 4'-phosphopantetheine of the acyl carrier protein (ACP) domain. {ECO0000269|PubMed16215233, ECO0000269|PubMed16969344, ECO0000269|PubMed26851298, ECO0000269|PubMed7567999, ECO0000269|PubMed8962082, ECO0000269|PubMed9356448}.
***Cdca3*:** Human Uniprot function (Human *CDCA3*): F-box-like protein that is required for entry into mitosis. Acts by participating in E3 ligase complexes that mediate the ubiquitination and degradation of WEE1 kinase at G2/M phase (by similarity). {ECO0000250}.
***Pck1*:** Human Uniprot function (Human *PCK1*): Cytosolic phosphoenolpyruvate carboxykinase that catalyzes the reversible decarboxylation and phosphorylation of oxaloacetate (OAA) and acts as the rate-limiting enzyme in gluconeogenesis (PubMed30193097, PubMed24863970, PubMed26971250, PubMed28216384). Regulates cataplerosis and anaplerosis, the processes that control the levels of metabolic intermediates in the citric acid cycle (PubMed30193097, PubMed24863970, PubMed26971250, PubMed28216384). At low glucose levels, it catalyzes the cataplerotic conversion of oxaloacetate to phosphoenolpyruvate (PEP), the rate-limiting step in the metabolic pathway that produces glucose from lactate and other precursors derived from the citric acid cycle (PubMed30193097). At high glucose levels, it catalyzes the anaplerotic conversion of phosphoenolpyruvate to oxaloacetate (PubMed30193097). Acts as a regulator of formation and maintenance of memory CD8(+) T-cells upregulated in these cells, where it generates phosphoenolpyruvate, via gluconeogenesis (by similarity). The resultant phosphoenolpyruvate flows to glycogen and pentose phosphate pathway, which is essential for memory CD8(+) T-cells homeostasis (by similarity). In addition to the phosphoenolpyruvate carboxykinase activity, also acts as a protein kinase when phosphorylated at Ser-90 phosphorylation at Ser-90 by AKT1 reduces the binding affinity to oxaloacetate and promotes an atypical serine protein kinase activity using GTP as donor (PubMed32322062). The protein kinase activity regulates lipogenesis upon phosphorylation at Ser-90, translocates to the endoplasmic reticulum and catalyzes phosphorylation of INSIG proteins (INSIG1 and INSIG2), thereby disrupting the interaction between INSIG proteins and SCAP and promoting nuclear translocation of SREBP proteins (SREBF1/SREBP1 or SREBF2/SREBP2) and subsequent transcription of downstream lipogenesis-related genes (PubMed32322062). {ECO0000250|UniProtKBQ9Z2V4, ECO0000269|PubMed24863970, ECO0000269|PubMed26971250, ECO0000269|PubMed28216384, ECO0000269|PubMed30193097, ECO0000269|PubMed32322062}.
***Slc10a1*:** Human Uniprot function (Human *SLC10A1*): The hepatic sodium/bile acid uptake system exhibits broad substrate specificity and transports various non-bile acid organic compounds as well. It is strictly dependent on the extracellular presence of sodium. FUNCTION (Microbial infection) Acts as a receptor for hepatitis B virus. {ECO0000269|PubMed23150796}.
***Cyp2c24*:** Human Uniprot function (Human *CYP2C18*): Cytochromes P450 are a group of heme-thiolate monooxygenases. In liver microsomes, this enzyme is involved in an NADPH-dependent electron transport pathway. It oxidizes a variety of structurally unrelated compounds, including steroids, fatty acids, and xenobiotics.
***Ube2t*:** Human Uniprot function (Human *UBE2T*): Accepts ubiquitin from the E1 complex and catalyzes its covalent attachment to other proteins. Catalyzes monoubiquitination. Involved in mitomycin-C (MMC)-induced DNA repair. Acts as a specific E2 ubiquitin-conjugating enzyme for the Fanconi anemia complex by associating with E3 ubiquitin-protein ligase FANCL and catalyzing monoubiquitination of FANCD2, a key step in the DNA damage pathway (PubMed16916645, PubMed17938197, PubMed19111657, PubMed19589784, PubMed28437106). Also mediates monoubiquitination of FANCL and FANCI

(PubMed16916645, PubMed17938197, PubMed19111657, PubMed19589784). May contribute to ubiquitination and degradation of BRCA1 (PubMed19887602). In vitro able to promote polyubiquitination using all seven ubiquitin Lys residues but may prefer 'Lys-11'-, 'Lys-27'-, 'Lys-48'- and 'Lys-63'-linked polyubiquitination (PubMed20061386). {ECO0000269|PubMed16916645, ECO0000269|PubMed17938197, ECO0000269|PubMed19111657, ECO0000269|PubMed19589784, ECO0000269|PubMed19887602, ECO0000269|PubMed20061386, ECO0000269|PubMed28437106}.
***Ckap2*:** Human Uniprot function (Human *CKAP2*): Possesses microtubule stabilizing properties. Involved in regulating aneuploidy, cell cycling, and cell death in a p53/TP53-dependent manner (by similarity). {ECO0000250}.
***Lilra3*:** Human Uniprot function (Human *LILRA6*): May act as receptor for class I MHC antigens. LIRA6_HUMAN,Q6PI73
***Lilrb3l*:** Human Uniprot function (Human *LILRA5*): May play a role in triggering innate immune responses. Does not seem to play a role for any class I MHC antigen recognition. {ECO:0000269|PubMed:16675463}.

Summary

Perfluorohexanesulfonamide (PFHxSAm) is a member of the per- and polyfluoroalkyl class of compounds to which humans are widely exposed. A review of the literature did not identify toxicological data for estimating the potential adverse health effects of PFHxSAm. This study used a transcriptomic approach and standard toxicological endpoints to estimate the in vivo biological potency of PFHxSAm.

A subset of standard toxicological endpoints (cholesterol concentration and neutrophil count in male rats; sorbitol dehydrogenase activity, total thyroxine concentration, and aspartate aminotransferase activity in female rats) exhibited benchmark dose (BMD) values much lower than would be expected given the endpoint-specific no-observed-effect level and lowest-observed-effect level values. Expert review of the data suggests that the BMD estimates do not accurately reflect the true potency of the effect of these endpoints and were likely an anomalous product of the BMD modeling approach.

Taking this into account, the most sensitive apical endpoint in male rats was a decrease in total thyroxine concentration with an estimated BMD and benchmark dose lower confidence limit (BMD_L) of 7.264 (5.024) mg/kg. Increases in absolute and relative liver weights were the next most sensitive apical endpoint changes observed in male rats with BMDs (BMD_Ls) of 8.492 (5.426) and 16.251 (8.358) mg/kg, respectively. In female rats, there were no apical endpoints for which a BMD value could be reliably estimated.

Gene set-level transcriptional changes in the liver following PFHxSAm exposure were estimated to occur at a BMD (BMD_L) as low as 0.520 (0.160) mg/kg in male rats, corresponding to negative regulation of myeloid cell differentiation (GO:0045638), and as low as 11.677 (5.931) mg/kg in female rats, corresponding to phenol-containing compound metabolic process (GO:0018958). The most sensitive liver gene for which a reliable BMD could be determined in male rats was *Egr1* with a BMD (BMD_L) of 0.750 (0.186) mg/kg, and *A2m* and *Loc100911545*/*A2m* in female rats, both with a BMD (BMD_L) of 1.163 (0.179) mg/kg.

Gene set-level transcriptional changes in the kidney were estimated to occur at a BMD (BMD_L) as low as 8.745 (5.224) mg/kg in male rats, corresponding to fat cell differentiation (GO:0045444), and as low as 10.324 (7.461) mg/kg in female rats, corresponding to regulation of cell division (GO:0051302). The most sensitive kidney gene for which a reliable BMD could be determined was *Loc100911814*/*Spink1l* with a BMD (BMD_L) of 0.510 (0.212) mg/kg in male rats and *Cdca3* with a BMD (BMD_L) of 2.619 (0.978) mg/kg in female rats.

Under the conditions of this short-duration transcriptomic study in Sprague Dawley (Hsd:Sprague Dawley® SD®) rats, the most sensitive point of departure with a reliable estimate in male rats was a transcriptional change in a gene, *Loc100911814*/*Spink1l* with a BMD (BMD_L) of 0.510 (0.212) mg/kg. Gene set transcriptional changes provided potency estimates in the same range, while apical endpoints provided potency estimates higher than *Loc100911814*/*Spink1l*. In female rats, the most sensitive point of departure with a reliable estimate was a transcriptional change in the genes *A2m* and *Loc100911545*/*A2m*, both with a BMD (BMD_L) of 1.163 (0.179) mg/kg. Gene set transcriptional changes provided potency estimates slightly higher than those of *A2m* and *Loc100911545*/*A2m*, while there were no apical endpoints with potency estimates that could be compared to *A2m* and *Loc100911545*/*A2m*.

References

1. U.S. Environmental Protection Agency (USEPA). CompTox Chemicals Dashboard: Perfluorohexanesulfonamide 41997-13-1 | DTXSID50469320. 2021. https://comptox.epa.gov/dashboard/chemical/details/DTXSID50469320

2. National Center for Biotechnology Information (NCBI). PubChem Compound Summary for CID 11603678, Perfluorohexanesulfonamide. 2021. https://pubchem.ncbi.nlm.nih.gov/compound/11603678

3. European Chemicals Agency (ECHA). Substance Infocard: Perfluorohexanesulfonamide. 2021. https://echa.europa.eu/substance-information/-/substanceinfo/100.250.649

4. Fenton SE, Ducatman A, Boobis A, DeWitt JC, Lau C, Ng C, Smith JS, Roberts SM. Per- and polyfluoroalkyl substance toxicity and human health review: Current state of knowledge and strategies for informing future research. Environ Toxicol Chem. 2021; 40(3):606-630. https://doi.org/10.1002/etc.4890

5. Domingo JL, Nadal M. Human exposure to per- and polyfluoroalkyl substances (PFAS) through drinking water: A review of the recent scientific literature. Environ Res. 2019; 177:108648. https://doi.org/10.1016/j.envres.2019.108648

6. Domingo JL, Nadal M. Per- and polyfluoroalkyl substances (PFASs) in food and human dietary intake: A review of the recent scientific literature. J Agric Food Chem. 2017; 65(3):533-543. https://doi.org/10.1021/acs.jafc.6b04683

7. U.S. Environmental Protection Agency (USEPA). CompTox Chemicals Dashboard: Perfluorohexanesulfonamide 41997-13-1 | DTXSID50469320: Exposure Predictions. 2021. https://comptox.epa.gov/dashboard/chemical/exposure-predictions/DTXSID50469320

8. U.S. Environmental Protection Agency (USEPA). CompTox Chemicals Dashboard: Perfluorohexanesulfonamide 41997-13-1 | DTXSID50469320: Executive Summary. 2021. https://comptox.epa.gov/dashboard/chemical/executive-summary/DTXSID50469320

9. Gwinn WM, Auerbach SS, Parham F, Stout MD, Waidyanatha S, Mutlu E, Collins B, Paules RS, Merrick BA, Ferguson S et al. Evaluation of 5-day in vivo rat liver and kidney with high-throughput transcriptomics for estimating benchmark doses of apical outcomes. Toxicol Sci. 2020; 176(2):343-354. https://doi.org/10.1093/toxsci/kfaa081

10. Mansouri K, Karmaus AL, Fitzpatrick J, Patlewicz G, Pradeep P, Alberga D, Alepee N, Allen TEH, Allen D, Alves VM et al. CATMoS: Collaborative Acute Toxicity Modeling Suite. Environ Health Perspect. 2021; 129(4):47013. https://doi.org/10.1289/EHP8495

11. Mansouri K, Grulke CM, Judson RS, Williams AJ. OPERA models for predicting physicochemical properties and environmental fate endpoints. J Cheminform. 2018; 10(1):10. https://doi.org/10.1186/s13321-018-0263-1

12. Patlewitz G. Personal Communication: EPA Point of Departure Estimate. 2021.

13. Waidyanatha S, Fletcher BL, Fernando RA, Cora MC, Silinski MAR. Development and validation of an ultraperformance liquid chromatography-tandem mass spectrometry method for quantitation of total 3,3',5-triiodo-L-thyronine and 3,3',5,5'-tetraiodo-L-thyronine in rodent serum. Anal Lett. 2021; 55(5):796-811. https://doi.org/10.1080/00032719.2021.1967969

14. Langmead B, Trapnell C, Pop M, Salzberg SL. Ultrafast and memory-efficient alignment of short DNA sequences to the human genome. Genome Biol. 2009; 10(3):R25. https://doi.org/10.1186/gb-2009-10-3-r25

15. Williams DA. A test for differences between treatment means when several dose levels are compared with a zero dose control. Biometrics. 1971; 27(1):103-117. http://dx.doi.org/10.2307/2528930

16. Williams DA. The comparison of several dose levels with a zero dose control. Biometrics. 1972; 28(2):519-531. http://dx.doi.org/10.2307/2556164

17. Dunnett CW. A multiple comparison procedure for comparing several treatments with a control. J Am Stat Assoc. 1955; 50(272):1096-1121. http://dx.doi.org/10.1080/01621459.1955.10501294

18. Shirley E. A non-parametric equivalent of Williams' test for contrasting increasing dose levels of a treatment. Biometrics. 1977; 33(2):386-389. http://dx.doi.org/10.2307/2529789

19. Dunn OJ. Multiple comparisons using rank sums. Technometrics. 1964; 6(3):241-252. http://dx.doi.org/10.1080/00401706.1964.10490181

20. Jonckheere AR. A distribution-free k-sample test against ordered alternatives. Biometrika. 1954; 41(1/2):133-145. http://dx.doi.org/10.2307/2333011

21. Dixon WJ, Massey FJ. Introduction to Statistical Analysis. New York,: McGraw-Hill; 1951.

22. U.S. Environmental Protection Agency (USEPA). Benchmark dose technical guidance. Washington, DC: U.S. Environmental Protection Agency, Risk Assessment Forum; 2012. https://www.epa.gov/sites/production/files/2015-01/documents/benchmark_dose_guidance.pdf

23. Wignall JA, Shapiro AJ, Wright FA, Woodruff TJ, Chiu WA, Guyton KZ, Rusyn I. Standardizing benchmark dose calculations to improve science-based decisions in human health assessments. Environ Health Perspect. 2014; 122(5):499-505. http://dx.doi.org/10.1289/ehp.1307539

24. National Toxicology Program (NTP). NTP research report on National Toxicology Program approach to genomic dose-response modeling. Research Triangle Park, NC: U.S. Department of Health and Human Services, National Institute of Environmental Health Sciences, National Toxicology Program; 2018. NTP Research Report No. 5.

25. Shi L, Jones WD, Jensen RV, Harris SC, Perkins RG, Goodsaid FM, Guo L, Croner LJ, Boysen C, Fang H et al. The balance of reproducibility, sensitivity, and specificity of lists of differentially expressed genes in microarray studies. BMC Bioinformatics. 2008; 9:S10. https://doi.org/10.1186/1471-2105-9-s9-s10

26. Auerbach SS, Aillon KL, Ballin JD, Collins BJ, Cora MC, Duncan NS, Fostel JM, Liu YF, Luh J, Machesky NJ et al. NIEHS report on the in vivo repeat dose biological potency study of 6:1 fluorotelomer alcohol (CASRN 375-82-6) in Sprague Dawley (Hsd:Sprague Dawley® SD®) rats (gavage studies). Research Triangle Park, NC: U.S. Department of Health and Human Services, Public Health Service, National Institute of Environmental Health Sciences; 2023. NIEHS Report 07. https://doi.org/10.22427/NIEHS-07

27. Auerbach SS, Ballin JD, Blake JC, Browning DB, Collins BJ, Cora MC, Fernando RA, Fostel JM, Liu YF, Luh J et al. NIEHS report on the in vivo repeat dose biological potency study of 1,1,2,2-tetrahydroperfluoro-1-dodecanol (CASRN 865-86-1) in Sprague Dawley (Hsd:Sprague Dawley® SD®) rats (gavage studies). Research Triangle Park, NC: U.S. Department of Health and Human Services, Public Health Service, National Institute of Environmental Health Sciences; 2023. NIEHS Report 08. https://doi.org/10.22427/NIEHS-08

28. Auerbach SS, Aillon KL, Ballin JD, Collins BJ, Cora MC, Duncan NS, Fostel JM, Kerns SP, Liu YF, Luh J et al. NIEHS report on the in vivo repeat dose biological potency study of 2,3-benzofluorene (CASRN 243-17-4) in Sprague Dawley (Hsd:Sprague Dawley® SD®) rats (gavage studies). Research Triangle Park, NC: U.S. Department of Health and Human Services, Public Health Service, National Institute of Environmental Health Sciences; 2023. NIEHS Report 09. https://doi.org/10.22427/NIEHS-09

29. National Toxicology Program (NTP). NIEHS 10: Chemical Effects in Biological Systems (CEBS) data repository. Research Triangle Park, NC: U.S. Department of Health and Human Services, National Institute of Environmental Health Sciences, National Toxicology Program; 2023. https://doi.org/10.22427/NIEHS-DATA-NIEHS-10

30. Geneontology. The gene ontology resource. 2021. http://geneontology.org/

31. Medical College of Wisconsin. Rat Genome Database. 2021. https://rgd.mcw.edu/

32. UniProt. UniProtKB results. 2021. https://www.uniprot.org/uniprot/

33. Entrez Gene. Gene. 2021. https://www.ncbi.nlm.nih.gov/gene/

34. Thomas RS, Allen BC, Nong A, Yang L, Bermudez E, Clewell HJ, III, Andersen ME. A method to integrate benchmark dose estimates with genomic data to assess the functional effects of chemical exposure. Toxicol Sci. 2007; 98(1):240-248. http://dx.doi.org/10.1093/toxsci/kfm092

Appendix A. Internal Dose Assessment

Table of Contents

A.1. Quantitation of Perfluorohexanesulfonamide in Plasma

Quantification of perfluorohexanesulfonamide (PFHxSAm) in plasma samples was completed by RTI International (Research Triangle, NC). An ultra-performance liquid chromatography-tandem mass spectrometry (UPLC-MS/MS) method was developed to determine PFHxSAm concentrations in rat plasma. A six-point matrix calibration curve, in the range of 10–1,000 ng/mL, was prepared by adding 10 µL of an appropriate spiking standard (PFHxSAm in methanol) and 10 µL of an internal standard solution (perfluoro-1-[13C8]octanesulfonamide in methanol) to 100 µL of control matrix (adult male Sprague Dawley rat plasma). Quality control (QC) samples were prepared similarly at a target concentration of 50 ng/mL in plasma. Blanks and study samples were prepared like calibration standards, except 10 µL of methanol was used in place of spiking solution. Sample extraction was achieved by adding 300 µL of acetonitrile, vortex mixing, and centrifuging for 10 minutes. A 10 µL aliquot from the supernatant of each sample was then diluted with 990 µL of 80/20 acetonitrile/water and mixed.

All samples were analyzed using a Waters Acquity UPLC (Milford, MA) coupled with an Applied Biosystems API-5000 mass detector (Framingham, MA). A Waters Acquity UPLC HSS T3 column (2.1 × 100 mm, 1.8 µm) and HSS T3 guard (2.1 × 5 mm, 1.8 µm) were used with mobile phases A (0.1% formic acid in water) and B (0.1% formic acid in acetonitrile). A flow rate of 0.3 mL/min was used with 1% B for 1 minute, a linear gradient of 1% to 99% B in 15 minutes, held for 4 minutes, reversed to 1% B in 0.5 minutes, and held for 1.5 minutes. The electrospray ion source was operated in the negative ion mode with a source temperature of 650°C and an ion spray voltage of −4500 V. Transition ranges monitored were m/z 398.0 to 78.0 (PFHxSAm quantitation ion) and m/z 506.0 to 78.0 (internal standard).

A linear regression with $1/X^2$ weighting was used to relate peak area ratios of analyte to internal standard and analyte concentrations. Calibration curves were linear ($r > 0.99$). The lower limit of quantitation (LOQ) for PFHxSAm in rat plasma was 10.0 ng/mL. For QC samples, the accuracy measured as percent relative error was within ±16.0% of the nominal concentration. The concentrations (ng/mL) of PFHxSAm in study samples were calculated using peak area ratios and the regression equation. Samples that had concentrations above the upper limit of the calibration curve were diluted and reanalyzed. All values were above the LOQ and were reported.

Appendix B. Animal Identifiers

Tables

Table B-1. Animal Numbers and FASTQ Data File Names

Animal Number	Sex	Group	Dose (mg/kg)	Survived to Study Termination	Tissue	FASTQ File ID
101	Male	Vehicle control	0	Yes	Kidney	Plate5-101
101	Male	Vehicle control	0	Yes	Liver	Plate1-101
102	Male	Vehicle control	0	Yes	Kidney	Plate5-102
102	Male	Vehicle control	0	Yes	Liver	Plate1-102
103	Male	Vehicle control	0	Yes	Kidney	Plate5-103
103	Male	Vehicle control	0	Yes	Liver	Plate1-103
104	Male	Vehicle control	0	Yes	Kidney	Plate5-104
104	Male	Vehicle control	0	Yes	Liver	Plate1-104
105	Male	Vehicle control	0	Yes	Kidney	Plate5-105
105	Male	Vehicle control	0	Yes	Liver	Plate1-105
106	Male	Vehicle control	0	Yes	Kidney	Plate5-106
106	Male	Vehicle control	0	Yes	Liver	Plate1-106
107	Male	Vehicle control	0	Yes	Kidney	Plate5-107
107	Male	Vehicle control	0	Yes	Liver	Plate1-107
108	Male	Vehicle control	0	Yes	Kidney	Plate5-108
108	Male	Vehicle control	0	Yes	Liver	Plate1-108
109	Male	Vehicle control	0	Yes	Kidney	Plate5-109
109	Male	Vehicle control	0	Yes	Liver	Plate1-109
110	Male	Vehicle control	0	Yes	Kidney	Plate5-110
110	Male	Vehicle control	0	Yes	Liver	Plate1-110
111	Female	Vehicle control	0	Yes	Kidney	Plate5-111
111	Female	Vehicle control	0	Yes	Liver	Plate1-111
112	Female	Vehicle control	0	Yes	Kidney	Plate5-112
112	Female	Vehicle control	0	Yes	Liver	Plate1-112
113	Female	Vehicle control	0	Yes	Kidney	Plate5-113
113	Female	Vehicle control	0	Yes	Liver	Plate1-113
114	Female	Vehicle control	0	Yes	Kidney	Plate5-114
114	Female	Vehicle control	0	Yes	Liver	Plate1-114
115	Female	Vehicle control	0	Yes	Kidney	Plate5-115
115	Female	Vehicle control	0	Yes	Liver	Plate1-115
116	Female	Vehicle control	0	Yes	Kidney	Plate5-116
116	Female	Vehicle control	0	Yes	Liver	Plate1-116
117	Female	Vehicle control	0	Yes	Kidney	Plate5-117
117	Female	Vehicle control	0	Yes	Liver	Plate1-117

Animal Number	Sex	Group	Dose (mg/kg)	Survived to Study Termination	Tissue	FASTQ File ID
118	Female	Vehicle control	0	Yes	Kidney	Plate5-118
118	Female	Vehicle control	0	Yes	Liver	Plate1-118
119	Female	Vehicle control	0	Yes	Kidney	Plate5-119
119	Female	Vehicle control	0	Yes	Liver	Plate1-119
120	Female	Vehicle control	0	Yes	Kidney	Plate5-120
120	Female	Vehicle control	0	Yes	Liver	Plate1-120
121	Male	Perfluorohexanesulfonamide	0.15	Yes	Kidney	Plate5-121
121	Male	Perfluorohexanesulfonamide	0.15	Yes	Liver	Plate1-121
122	Male	Perfluorohexanesulfonamide	0.15	Yes	Kidney	Plate5-122
122	Male	Perfluorohexanesulfonamide	0.15	Yes	Liver	Plate1-122
123	Male	Perfluorohexanesulfonamide	0.15	Yes	Kidney	Plate5-123
123	Male	Perfluorohexanesulfonamide	0.15	Yes	Liver	Plate1-123
124	Male	Perfluorohexanesulfonamide	0.15	Yes	Kidney	Plate5-124
124	Male	Perfluorohexanesulfonamide	0.15	Yes	Liver	Plate1-124
125	Male	Perfluorohexanesulfonamide	0.15	Yes	Kidney	Plate5-125
125	Male	Perfluorohexanesulfonamide	0.15	Yes	Liver	Plate1-125
126	Female	Perfluorohexanesulfonamide	0.15	Yes	Kidney	Plate5-126
126	Female	Perfluorohexanesulfonamide	0.15	Yes	Liver	Plate1-126
127	Female	Perfluorohexanesulfonamide	0.15	Yes	Kidney	Plate5-127
127	Female	Perfluorohexanesulfonamide	0.15	Yes	Liver	Plate1-127
128	Female	Perfluorohexanesulfonamide	0.15	Yes	Kidney	Plate5-128
128	Female	Perfluorohexanesulfonamide	0.15	Yes	Liver	Plate1-128
129	Female	Perfluorohexanesulfonamide	0.15	Yes	Kidney	Plate5-129
129	Female	Perfluorohexanesulfonamide	0.15	Yes	Liver	Plate1-129[a]
130	Female	Perfluorohexanesulfonamide	0.15	Yes	Kidney	Plate5-130
130	Female	Perfluorohexanesulfonamide	0.15	Yes	Liver	Plate1-130
131	Male	Perfluorohexanesulfonamide	0.5	Yes	Kidney	Plate5-131
131	Male	Perfluorohexanesulfonamide	0.5	Yes	Liver	Plate1-131
132	Male	Perfluorohexanesulfonamide	0.5	Yes	Kidney	Plate5-132
132	Male	Perfluorohexanesulfonamide	0.5	Yes	Liver	Plate1-132
133	Male	Perfluorohexanesulfonamide	0.5	Yes	Kidney	Plate5-133
133	Male	Perfluorohexanesulfonamide	0.5	Yes	Liver	Plate1-133
134	Male	Perfluorohexanesulfonamide	0.5	Yes	Kidney	Plate5-134
134	Male	Perfluorohexanesulfonamide	0.5	Yes	Liver	Plate1-134
135	Male	Perfluorohexanesulfonamide	0.5	Yes	Kidney	Plate5-135

Animal Number	Sex	Group	Dose (mg/kg)	Survived to Study Termination	Tissue	FASTQ File ID
135	Male	Perfluorohexanesulfonamide	0.5	Yes	Liver	Plate1-135
136	Female	Perfluorohexanesulfonamide	0.5	Yes	Kidney	Plate5-136
136	Female	Perfluorohexanesulfonamide	0.5	Yes	Liver	Plate1-136
137	Female	Perfluorohexanesulfonamide	0.5	Yes	Kidney	Plate5-137
137	Female	Perfluorohexanesulfonamide	0.5	Yes	Liver	Plate1-137
138	Female	Perfluorohexanesulfonamide	0.5	Yes	Kidney	Plate5-138
138	Female	Perfluorohexanesulfonamide	0.5	Yes	Liver	Plate1-138
139	Female	Perfluorohexanesulfonamide	0.5	Yes	Kidney	Plate5-139
139	Female	Perfluorohexanesulfonamide	0.5	Yes	Liver	Plate1-139
140	Female	Perfluorohexanesulfonamide	0.5	Yes	Kidney	Plate5-140
140	Female	Perfluorohexanesulfonamide	0.5	Yes	Liver	Plate1-140
141	Male	Perfluorohexanesulfonamide	1.4	Yes	Kidney	Plate5-141
141	Male	Perfluorohexanesulfonamide	1.4	Yes	Liver	Plate1-141
142	Male	Perfluorohexanesulfonamide	1.4	Yes	Kidney	Plate5-142
142	Male	Perfluorohexanesulfonamide	1.4	Yes	Liver	Plate1-142
143	Male	Perfluorohexanesulfonamide	1.4	Yes	Kidney	Plate5-143
143	Male	Perfluorohexanesulfonamide	1.4	Yes	Liver	Plate1-143
144	Male	Perfluorohexanesulfonamide	1.4	Yes	Kidney	Plate5-144
144	Male	Perfluorohexanesulfonamide	1.4	Yes	Liver	Plate1-144
145	Male	Perfluorohexanesulfonamide	1.4	Yes	Kidney	Plate5-145
145	Male	Perfluorohexanesulfonamide	1.4	Yes	Liver	Plate1-145
146	Female	Perfluorohexanesulfonamide	1.4	Yes	Kidney	Plate5-146
146	Female	Perfluorohexanesulfonamide	1.4	Yes	Liver	Plate1-146
147	Female	Perfluorohexanesulfonamide	1.4	Yes	Kidney	Plate5-147
147	Female	Perfluorohexanesulfonamide	1.4	Yes	Liver	Plate1-147
148	Female	Perfluorohexanesulfonamide	1.4	Yes	Kidney	Plate5-148
148	Female	Perfluorohexanesulfonamide	1.4	Yes	Liver	Plate1-148
149	Female	Perfluorohexanesulfonamide	1.4	Yes	Kidney	Plate5-149
149	Female	Perfluorohexanesulfonamide	1.4	Yes	Liver	Plate1-149
150	Female	Perfluorohexanesulfonamide	1.4	Yes	Kidney	Plate5-150
150	Female	Perfluorohexanesulfonamide	1.4	Yes	Liver	Plate1-150
151	Male	Perfluorohexanesulfonamide	4.0	Yes	Kidney	Plate5-151
151	Male	Perfluorohexanesulfonamide	4.0	Yes	Liver	Plate1-151
152	Male	Perfluorohexanesulfonamide	4.0	Yes	Kidney	Plate5-152
152	Male	Perfluorohexanesulfonamide	4.0	Yes	Liver	Plate1-152

Animal Number	Sex	Group	Dose (mg/kg)	Survived to Study Termination	Tissue	FASTQ File ID
153	Male	Perfluorohexanesulfonamide	4.0	Yes	Kidney	Plate5-153
153	Male	Perfluorohexanesulfonamide	4.0	Yes	Liver	Plate1-153
154	Male	Perfluorohexanesulfonamide	4.0	Yes	Kidney	Plate5-154
154	Male	Perfluorohexanesulfonamide	4.0	Yes	Liver	Plate1-154
155	Male	Perfluorohexanesulfonamide	4.0	Yes	Kidney	Plate5-155
155	Male	Perfluorohexanesulfonamide	4.0	Yes	Liver	Plate1-155
156	Female	Perfluorohexanesulfonamide	4.0	Yes	Kidney	Plate5-156
156	Female	Perfluorohexanesulfonamide	4.0	Yes	Liver	Plate1-156
157	Female	Perfluorohexanesulfonamide	4.0	Yes	Kidney	Plate5-157
157	Female	Perfluorohexanesulfonamide	4.0	Yes	Liver	Plate1-157
158	Female	Perfluorohexanesulfonamide	4.0	Yes	Kidney	Plate5-158
158	Female	Perfluorohexanesulfonamide	4.0	Yes	Liver	Plate1-158
159	Female	Perfluorohexanesulfonamide	4.0	Yes	Kidney	Plate5-159
159	Female	Perfluorohexanesulfonamide	4.0	Yes	Liver	Plate1-159
160	Female	Perfluorohexanesulfonamide	4.0	Yes	Kidney	Plate5-160
160	Female	Perfluorohexanesulfonamide	4.0	Yes	Liver	Plate1-160
161	Male	Perfluorohexanesulfonamide	12.0	Yes	Kidney	Plate5-161
161	Male	Perfluorohexanesulfonamide	12.0	Yes	Liver	Plate1-161
162	Male	Perfluorohexanesulfonamide	12.0	Yes	Kidney	Plate5-162
162	Male	Perfluorohexanesulfonamide	12.0	Yes	Liver	Plate1-162
163	Male	Perfluorohexanesulfonamide	12.0	Yes	Kidney	Plate5-163
163	Male	Perfluorohexanesulfonamide	12.0	Yes	Liver	Plate1-163
164	Male	Perfluorohexanesulfonamide	12.0	Yes	Kidney	Plate5-164
164	Male	Perfluorohexanesulfonamide	12.0	Yes	Liver	Plate1-164
165	Male	Perfluorohexanesulfonamide	12.0	Yes	Kidney	Plate5-165
165	Male	Perfluorohexanesulfonamide	12.0	Yes	Liver	Plate1-165
166	Female	Perfluorohexanesulfonamide	12.0	Yes	Kidney	Plate5-166
166	Female	Perfluorohexanesulfonamide	12.0	Yes	Liver	Plate1-166
167	Female	Perfluorohexanesulfonamide	12.0	Yes	Kidney	Plate5-167
167	Female	Perfluorohexanesulfonamide	12.0	Yes	Liver	Plate1-167
168	Female	Perfluorohexanesulfonamide	12.0	Yes	Kidney	Plate5-168
168	Female	Perfluorohexanesulfonamide	12.0	Yes	Liver	Plate1-168
169	Female	Perfluorohexanesulfonamide	12.0	Yes	Kidney	Plate5-169
169	Female	Perfluorohexanesulfonamide	12.0	Yes	Liver	Plate1-169
170	Female	Perfluorohexanesulfonamide	12.0	Yes	Kidney	Plate5-170

Animal Number	Sex	Group	Dose (mg/kg)	Survived to Study Termination	Tissue	FASTQ File ID
170	Female	Perfluorohexanesulfonamide	12.0	Yes	Liver	Plate1-170
171	Male	Perfluorohexanesulfonamide	37.0	Yes	Kidney	Plate5-171
171	Male	Perfluorohexanesulfonamide	37.0	Yes	Liver	Plate1-171
172	Male	Perfluorohexanesulfonamide	37.0	Yes	Kidney	Plate5-172
172	Male	Perfluorohexanesulfonamide	37.0	Yes	Liver	Plate1-172
173	Male	Perfluorohexanesulfonamide	37.0	Yes	Kidney	Plate5-173
173	Male	Perfluorohexanesulfonamide	37.0	Yes	Liver	Plate1-173
174	Male	Perfluorohexanesulfonamide	37.0	Yes	Kidney	Plate5-174
174	Male	Perfluorohexanesulfonamide	37.0	Yes	Liver	Plate1-174
175	Male	Perfluorohexanesulfonamide	37.0	Yes	Kidney	Plate5-175
175	Male	Perfluorohexanesulfonamide	37.0	Yes	Liver	Plate1-175
176	Female	Perfluorohexanesulfonamide	37.0	Yes	Kidney	Plate5-176
176	Female	Perfluorohexanesulfonamide	37.0	Yes	Liver	Plate1-176
177	Female	Perfluorohexanesulfonamide	37.0	Yes	Kidney	Plate5-177
177	Female	Perfluorohexanesulfonamide	37.0	Yes	Liver	Plate1-177
178	Female	Perfluorohexanesulfonamide	37.0	Yes	Kidney	Plate5-178
178	Female	Perfluorohexanesulfonamide	37.0	Yes	Liver	Plate1-178
179	Female	Perfluorohexanesulfonamide	37.0	Yes	Kidney	Plate5-179
179	Female	Perfluorohexanesulfonamide	37.0	Yes	Liver	Plate1-179
180	Female	Perfluorohexanesulfonamide	37.0	Yes	Kidney	Plate5-180
180	Female	Perfluorohexanesulfonamide	37.0	Yes	Liver	Plate1-180
181	Male	Perfluorohexanesulfonamide	111.0	Yes	Kidney	Plate5-181
181	Male	Perfluorohexanesulfonamide	111.0	Yes	Liver	Plate1-181
182	Male	Perfluorohexanesulfonamide	111.0	Yes	Kidney	Plate5-182
182	Male	Perfluorohexanesulfonamide	111.0	Yes	Liver	Plate1-182
183	Male	Perfluorohexanesulfonamide	111.0	Yes	Kidney	Plate5-183
183	Male	Perfluorohexanesulfonamide	111.0	Yes	Liver	Plate1-183
184	Male	Perfluorohexanesulfonamide	111.0	Yes	Kidney	Plate5-184
184	Male	Perfluorohexanesulfonamide	111.0	Yes	Liver	Plate1-184
185	Male	Perfluorohexanesulfonamide	111.0	Yes	Kidney	Plate5-185
185	Male	Perfluorohexanesulfonamide	111.0	Yes	Liver	Plate1-185
186	Female	Perfluorohexanesulfonamide	111.0	Yes	Kidney	Plate5-186
186	Female	Perfluorohexanesulfonamide	111.0	Yes	Liver	Plate1-186
187	Female	Perfluorohexanesulfonamide	111.0	Yes	Kidney	Plate5-187
187	Female	Perfluorohexanesulfonamide	111.0	Yes	Liver	Plate1-187

Animal Number	Sex	Group	Dose (mg/kg)	Survived to Study Termination	Tissue	FASTQ File ID
188	Female	Perfluorohexanesulfonamide	111.0	Yes	Kidney	Plate5-188
188	Female	Perfluorohexanesulfonamide	111.0	Yes	Liver	Plate1-188
189	Female	Perfluorohexanesulfonamide	111.0	Yes	Kidney	Plate5-189
189	Female	Perfluorohexanesulfonamide	111.0	Yes	Liver	Plate1-189
190	Female	Perfluorohexanesulfonamide	111.0	Yes	Kidney	Plate5-190
190	Female	Perfluorohexanesulfonamide	111.0	Yes	Liver	Plate1-190
191	Male	Perfluorohexanesulfonamide	333.0	No	None	NA
192	Male	Perfluorohexanesulfonamide	333.0	No	None	NA
193	Male	Perfluorohexanesulfonamide	333.0	No	None	NA
194	Male	Perfluorohexanesulfonamide	333.0	No	None	NA
195	Male	Perfluorohexanesulfonamide	333.0	No	None	NA
196	Female	Perfluorohexanesulfonamide	333.0	No	None	NA
197	Female	Perfluorohexanesulfonamide	333.0	No	None	NA
198	Female	Perfluorohexanesulfonamide	333.0	No	None	NA
199	Female	Perfluorohexanesulfonamide	333.0	No	None	NA
200	Female	Perfluorohexanesulfonamide	333.0	No	None	NA
201	Male	Perfluorohexanesulfonamide	1,000.0	No	None	NA
202	Male	Perfluorohexanesulfonamide	1,000.0	No	None	NA
203	Male	Perfluorohexanesulfonamide	1,000.0	No	None	NA
204	Male	Perfluorohexanesulfonamide	1,000.0	No	None	NA
205	Male	Perfluorohexanesulfonamide	1,000.0	No	None	NA
206	Female	Perfluorohexanesulfonamide	1,000.0	No	None	NA
207	Female	Perfluorohexanesulfonamide	1,000.0	No	None	NA
208	Female	Perfluorohexanesulfonamide	1,000.0	No	None	NA
209	Female	Perfluorohexanesulfonamide	1,000.0	No	None	NA
210	Female	Perfluorohexanesulfonamide	1,000.0	No	None	NA

NA = no transcriptomics data collected for selected animal.
[a]Removed due to principal component analysis/hierarchical cluster analysis outlier.

Appendix C. Transcriptomic Quality Control and Empirical False Discovery Rate

Table of Contents

Tables

Figures

C.1. Gene Expression Quality Control

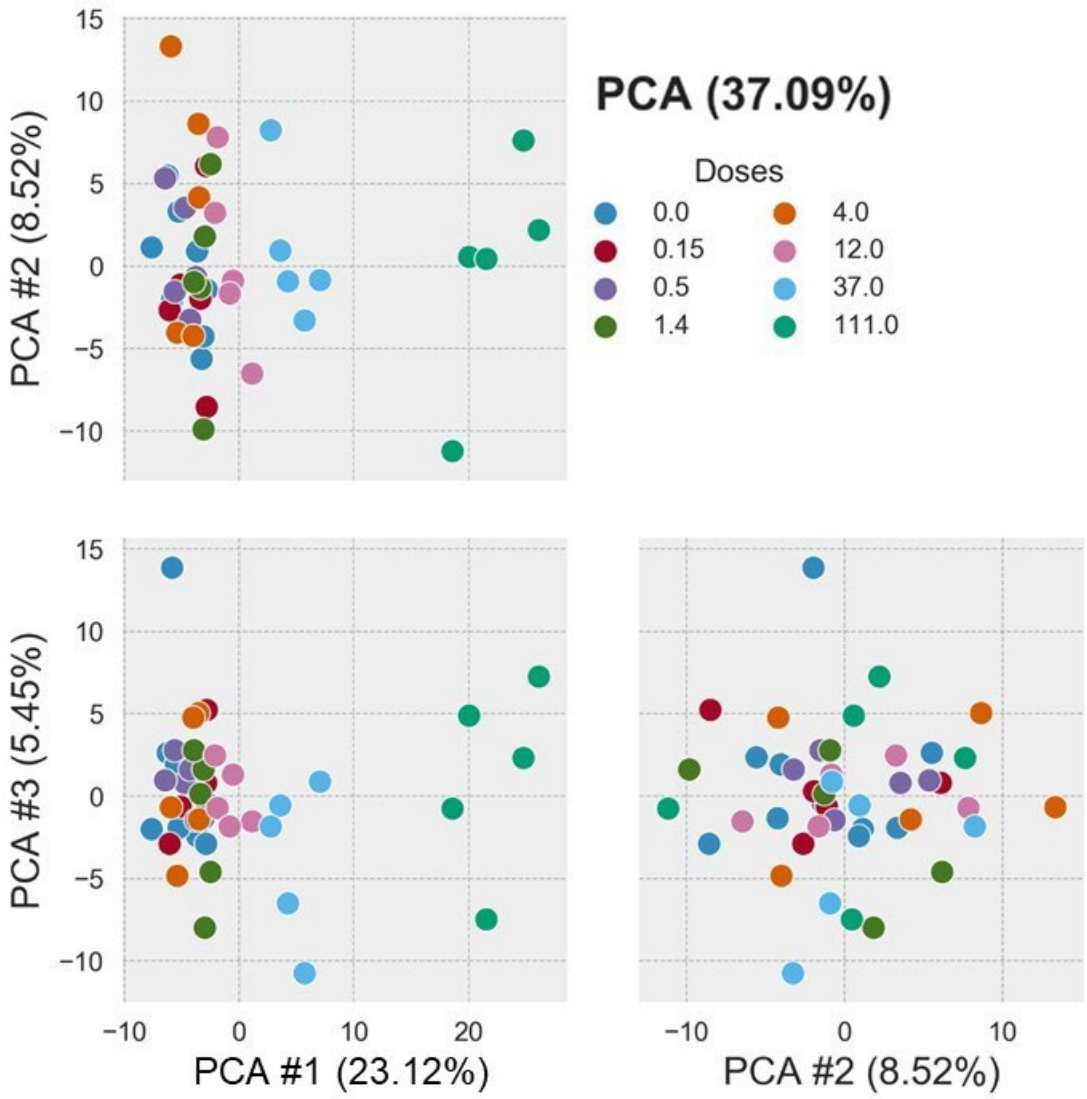

Figure C-1. A Principal Component Analysis of the Normalized Data from the Liver of Male Rats

A principal component analysis (PCA) plot enables visualization of global transcriptional changes in two dimensions, with each plot showing a different angle on the basis of the principal components plotted. Global transcript data are shown for individual animals (dots) within each dose group (designated by color). Dots that are spatially closer to each other indicate more similarity in global expression profiles; dots that are farther apart indicate dissimilarity in global expression profiles for those animals. The data represented in the plot are those employed in dose response modeling (i.e., if outliers were identified in the quality control process, they were removed from the data set and are not present in the plot). Visual inspection does not suggest subgrouping of the data other than dose-related changes, which indicates any technical batch-related effects are minimal.

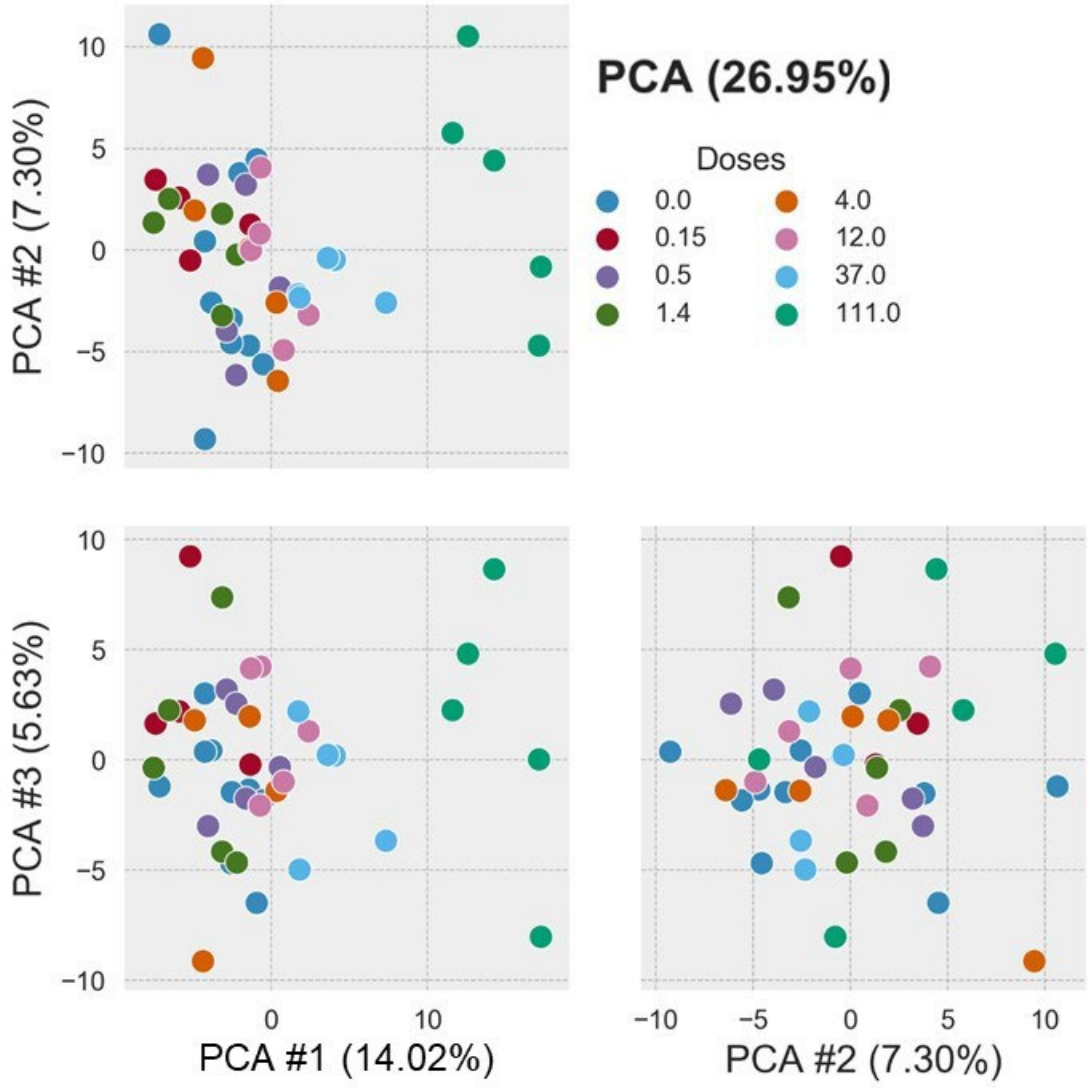

Figure C-2. A Principal Component Analysis of the Normalized Data from the Liver of Female Rats

A principal component analysis (PCA) plot enables visualization of global transcriptional changes in two dimensions, with each plot showing a different angle on the basis of the principal components plotted. Global transcript data are shown for individual animals (dots) within each dose group (designated by color). Dots that are spatially closer to each other indicate more similarity in global expression profiles; dots that are farther apart indicate dissimilarity in global expression profiles for those animals. The data represented in the plot are those employed in dose response modeling (i.e., if outliers were identified in the quality control process, they were removed from the data set and are not present in the plot). Visual inspection does not suggest subgrouping of the data other than dose-related changes, which indicates any technical batch-related effects are minimal.

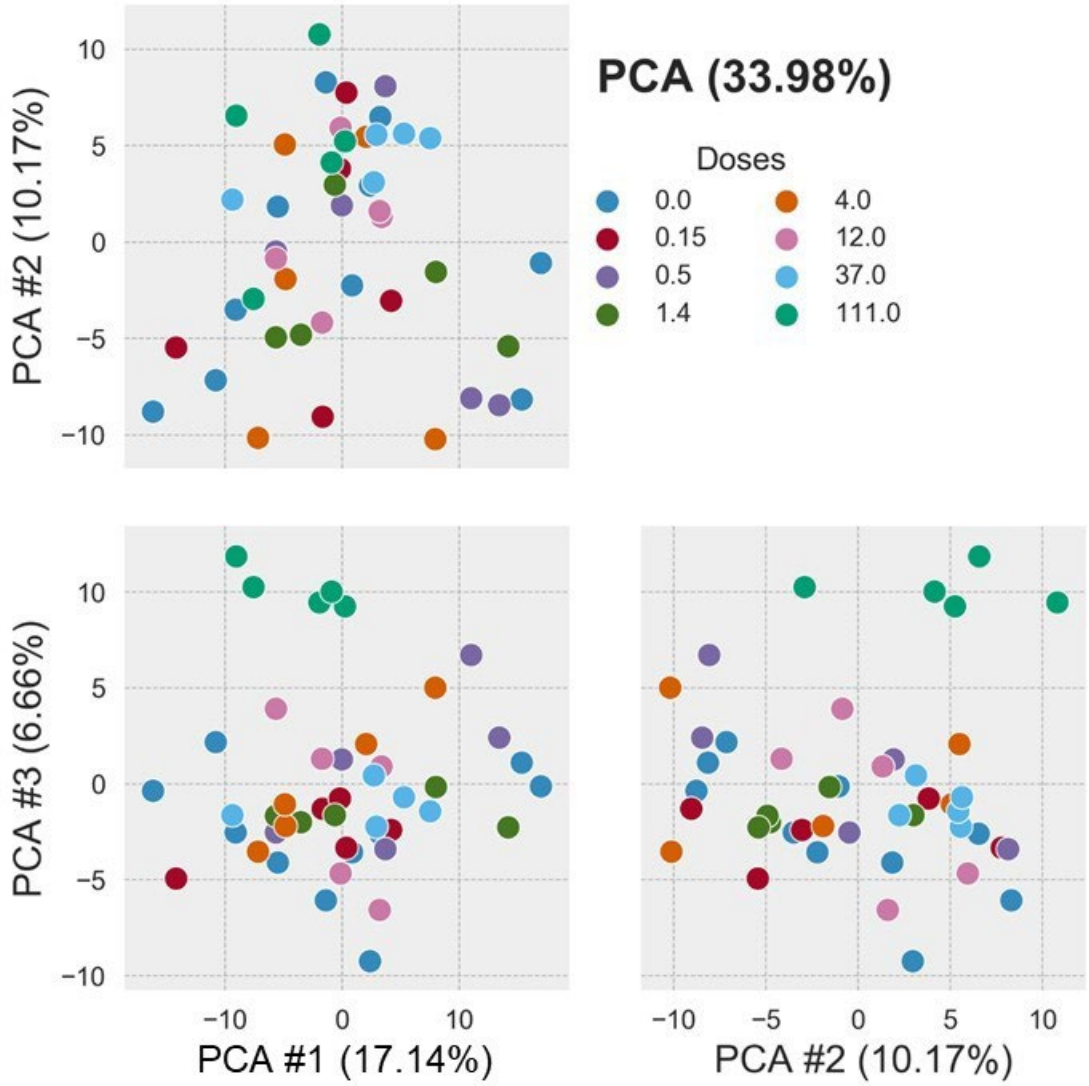

Figure C-3. A Principal Component Analysis of the Normalized Data from the Kidney of Male Rats

A principal component analysis (PCA) plot enables visualization of global transcriptional changes in two dimensions, with each plot showing a different angle on the basis of the principal components plotted. Global transcript data are shown for individual animals (dots) within each dose group (designated by color). Dots that are spatially closer to each other indicate more similarity in global expression profiles; dots that are farther apart indicate dissimilarity in global expression profiles for those animals. The data represented in the plot are those employed in dose response modeling (i.e., if outliers were identified in the quality control process, they were removed from the data set and are not present in the plot). Visual inspection does not suggest subgrouping of the data other than dose-related changes, which indicates any technical batch-related effects are minimal.

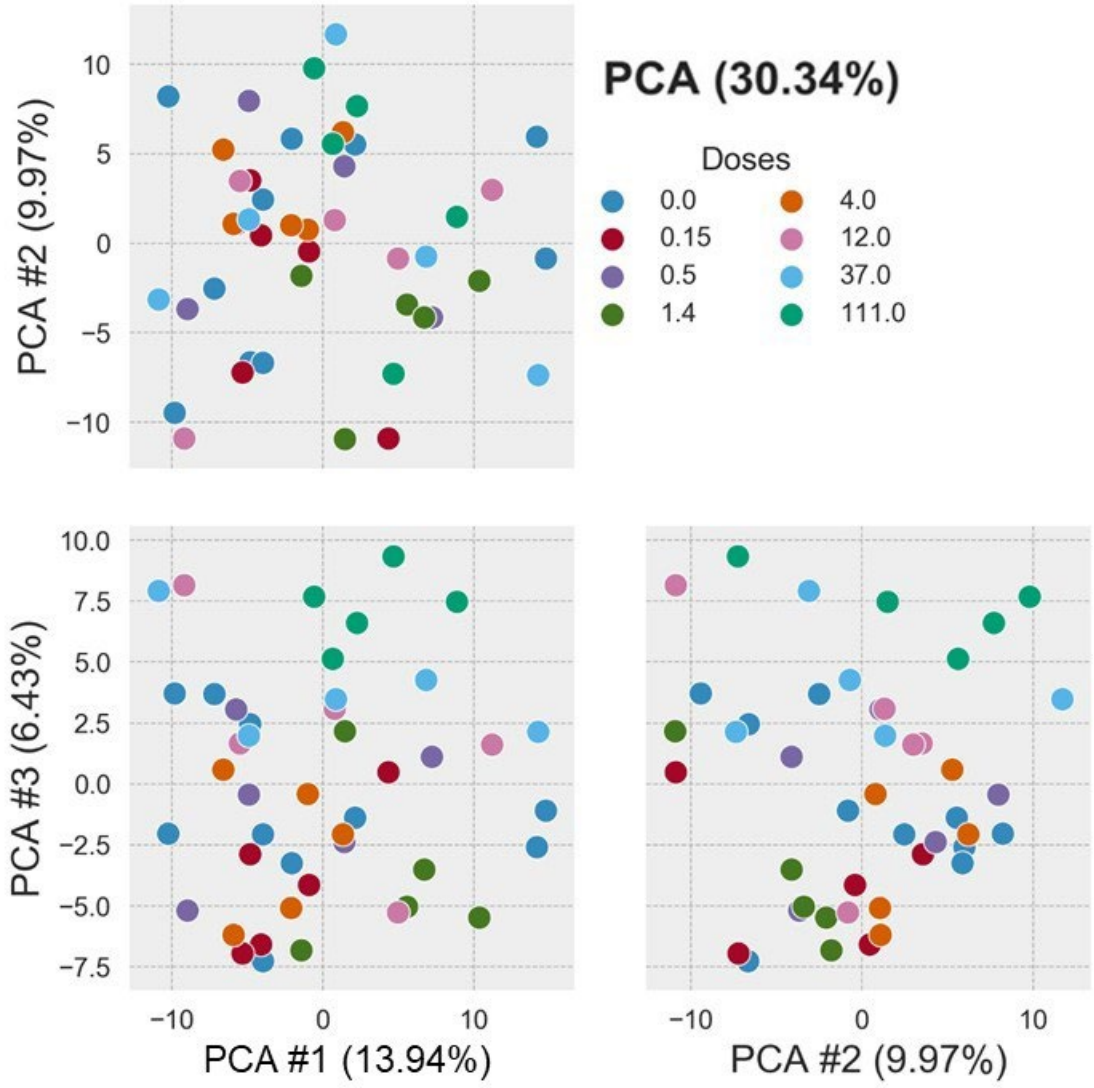

Figure C-4. A Principal Component Analysis of the Normalized Data from the Kidney of Female Rats

A principal component analysis (PCA) plot enables visualization of global transcriptional changes in two dimensions, with each plot showing a different angle on the basis of the principal components plotted. Global transcript data are shown for individual animals (dots) within each dose group (designated by color). Dots that are spatially closer to each other indicate more similarity in global expression profiles; dots that are farther apart indicate dissimilarity in global expression profiles for those animals. The data represented in the plot are those employed in dose response modeling (i.e., if outliers were identified in the quality control process, they were removed from the data set and are not present in the plot). Visual inspection does not suggest subgrouping of the data other than minor dose-related changes, which indicates any technical batch-related effects are minimal.

C.2. Empirical False Discovery Rate

C.2.1. Methods

Empirical false discovery assessment was performed to evaluate the performance of the benchmark dose (BMD) analysis technique and underlining probe/pathway filtering criteria. Toward this goal, 20 computationally generated data sets were used with this study design (each data set containing 10 vehicle control replicates and 5 replicates per dose), and equivalent BMD analysis was performed using the same parameter configurations. The 20 data sets were generated from the original perfluorohexanesulfonamide (PFHxSAm) study data, along with data from three other chemicals that were studied in parallel under a similar protocol.[26-28]

For a given group (tissue per sex combination), up to 40 vehicle control samples from the original studies (10 replicates × 4 chemicals) were used for this analysis. The previously identified outlier vehicle control samples and overflow plate control samples exhibiting a batch effect were excluded from this analysis.

Each computationally generated sample was created by randomly mixing the normalized expression signal from two randomly selected vehicle control samples using a weighted average approach. The weights utilized during per-probe mixing were randomly simulated from uniform (0,1) distribution. A total of 55 samples (10 vehicle control samples + 45 dosed samples [9 doses × 5 replicates]) were computationally generated per data set and assigned to either vehicle control or 1 of the 9 dosed groups that were separated by approximately half-log spacing, consistent with the dose spacing used in the original studies. For each group, 20 such data sets were generated. Because each of the 20 generated data sets used in the empirical false discovery analysis was derived from actual vehicle control samples, none of the data sets should have any true dose-responsive genes.

Each data set was then analyzed using the same parameter settings and significance criteria that were implemented in the original study. At the gene level, genes that passed the following criteria were considered false positive discoveries: fold change ≥|2|, Williams's trend p value ≤0.05, global goodness-of-fit p value >0.1, BMD upper confidence limit/BMD lower confidence limit (BMD_U/BMD_L) ≤40, and BMD <highest dose tested. Categorical analysis on Gene Ontology (GO) gene sets was performed using the genes that passed the gene-level criteria with maximum absolute fold change ≥1.5. At the gene set GO level, GO biological processes that passed the following criteria were considered false positive discoveries: ≥3 genes that pass all filters, totaling at least 5% of the genes in a gene set.

False positive discovery rates were assessed for each computationally generated data set using the following equations:

$$\text{False Positive Gene Rate} = \frac{\text{\# False Positive Entrez Gene IDs}}{2{,}680} \times 100 \quad (1)$$

$$\text{False Positive GO Biological Process Rate} = \frac{\text{\# False Positive GO Biological Processes}}{5{,}667} \times 100 \quad (2)$$

where 2,680 is the number of unique Entrez Gene IDs on the rat S1500+ platform and 5,667 is the number of GO biological processes that have at least three genes in rat S1500+.

Mean and median false discovery rates across all 20 computationally generated data sets were calculated for each tissue per sex in the study.

C.2.2. Results

The number of false positives for genes and GO biological processes are given in Table C-1. Mean and median false positive rates were <0.1% for genes and <0.5% for GO biological processes for all tissue per sex group (Figure C-5 and Figure C-6). The maximum false positive rates for any of the 80 computationally generated control data sets were 0.3% (gene) and 4.4% (GO biological process).

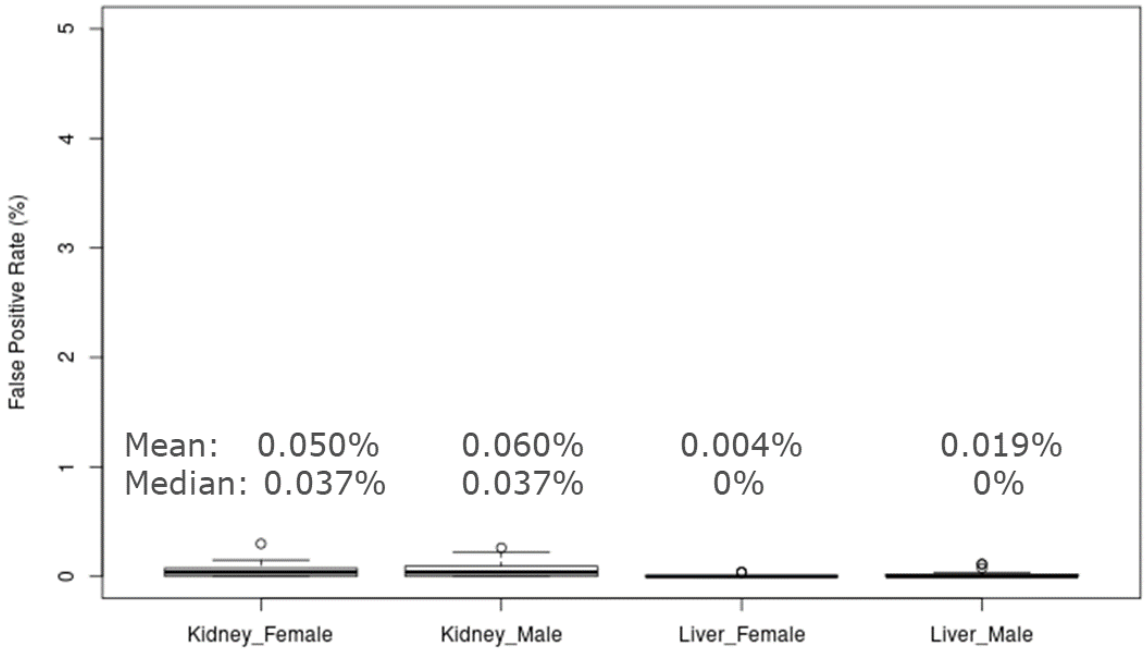

Figure C-5. Boxplots of the False Positive Gene Rate for Each Tissue per Sex Combination

Each boxplot displays the distribution of the false positive rates for 20 computationally generated data sets.

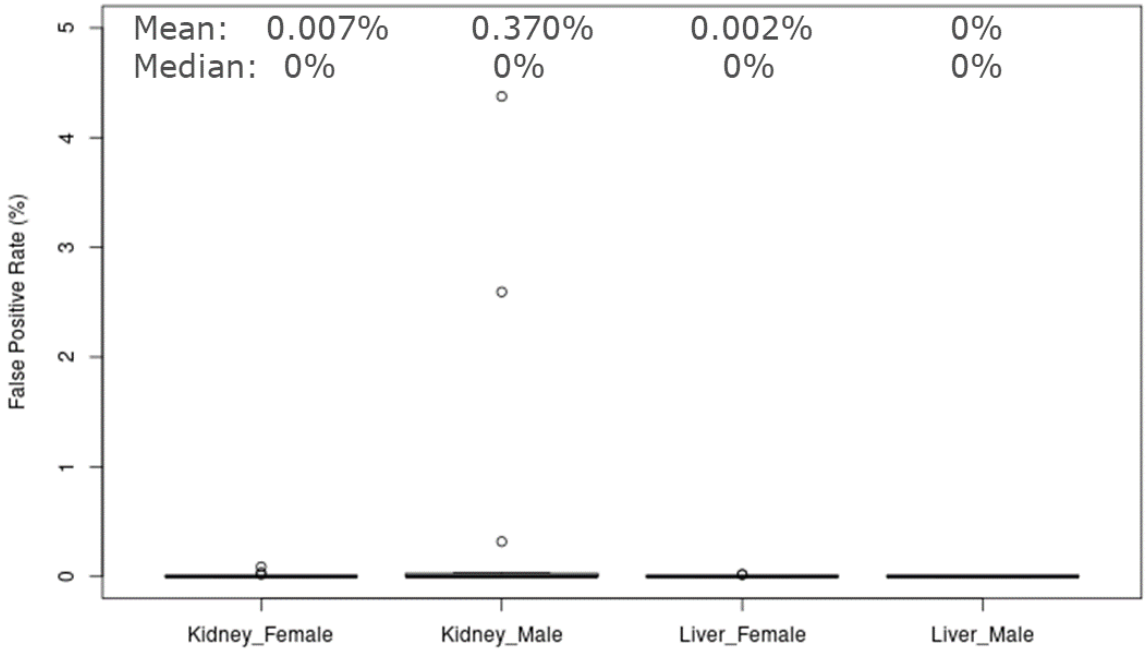

Figure C-6. Boxplots of the False Positive Gene Ontology Biological Process Rate for Each Tissue per Sex Combination

Each boxplot displays the distribution of the false positive rates for 20 computationally generated data sets.

Table C-1. Number of False Positives

Generated Data Set	# False Positive Genes				# False Positive GO Biological Process			
	Kidney Female	Kidney Male	Liver Female	Liver Male	Kidney Female	Kidney Male	Liver Female	Liver Male
01	3	0	0	0	0	0	0	0
02	4	0	0	0	2	1	0	0
03	0	2	0	0	0	1	1	0
04	2	1	0	0	0	0	0	0
05	2	3	0	0	0	0	0	0
06	1	0	0	3	0	0	1	0
07	1	6	0	0	0	18	0	0
08	0	0	0	0	0	0	0	0
09	3	0	0	0	0	0	0	0
10	0	0	0	0	0	0	0	0
11	0	1	0	1	0	0	0	0
12	1	4	0	3	1	147	0	0
13	0	2	0	0	0	2	0	0
14	1	0	0	2	0	0	0	0
15	0	3	0	0	0	2	0	0

Generated Data Set	# False Positive Genes				# False Positive GO Biological Process			
	Kidney Female	Kidney Male	Liver Female	Liver Male	Kidney Female	Kidney Male	Liver Female	Liver Male
16	0	1	1	0	0	0	0	0
17	0	0	1	0	0	0	0	0
18	0	2	0	0	0	0	0	0
19	1	0	0	1	0	0	0	0
20	8	7	0	0	5	248	0	0

GO = Gene Ontology.

Appendix D. Benchmark Dose Model Recommendation and Selection Methodologies

Tables

Figures

Table D-1. Benchmark Dose Model Recommendation/Selection Rules for Apical Endpoints

Rule	Criteria for "Viable"	Numerical Threshold	Bin Placement for Rule Failure
BMD Existence	A BMD exists.	NA	Failure
BMD_L Existence	A BMD_L exists.	NA	Failure
AIC Existence	An AIC exists.	NA	Failure
Residual of Interest Existence	The residual at the dose group closest to the BMD (i.e., the residual of interest) exists.	NA	Failure
Variance Model Fit	The variance model used fits the data.	NA	Nonviable
Variance Model Selection	The variance model is appropriate.	NA	Nonviable
Global Goodness of Fit	The mean model fits the data means sufficiently well (BMDS 2.7.0 Test 4 p value >N).	0.1	Nonviable
Degrees of Freedom	There is at least 1 degree of freedom (i.e., more dose groups than model parameters).	NA	Nonviable
BMD-to-BMD_L Ratio	The ratio of BMD to BMD_L is not large (BMD/BMD_L <N).	20	Viable
High BMD_L	The BMD_L is <N times higher than the maximum dose.	1	Viable
High BMD	The BMD is <N times higher than the maximum dose.	1	Viable
Low BMD	The BMD is <N times lower than the minimum nonzero dose.	3	Nonreportable
Control Residual	The residual at control is small (residual <N).	2	Nonviable
Control Standard Deviation	The modeled standard deviation is similar to the actual (<N times different).	1.5	Nonviable
Residual of Interest	The residual at the dose group closest to the BMD (i.e., the residual of interest) is small (residual <N).	2	Nonviable
No Warnings Reported	No warnings in the BMD model system were reported.	NA	Viable

BMD = benchmark dose; NA = not applicable; BMD_L = benchmark dose lower confidence limit; AIC = Akaike information criterion; BMDS = Benchmark Dose Software; N = numerical threshold.

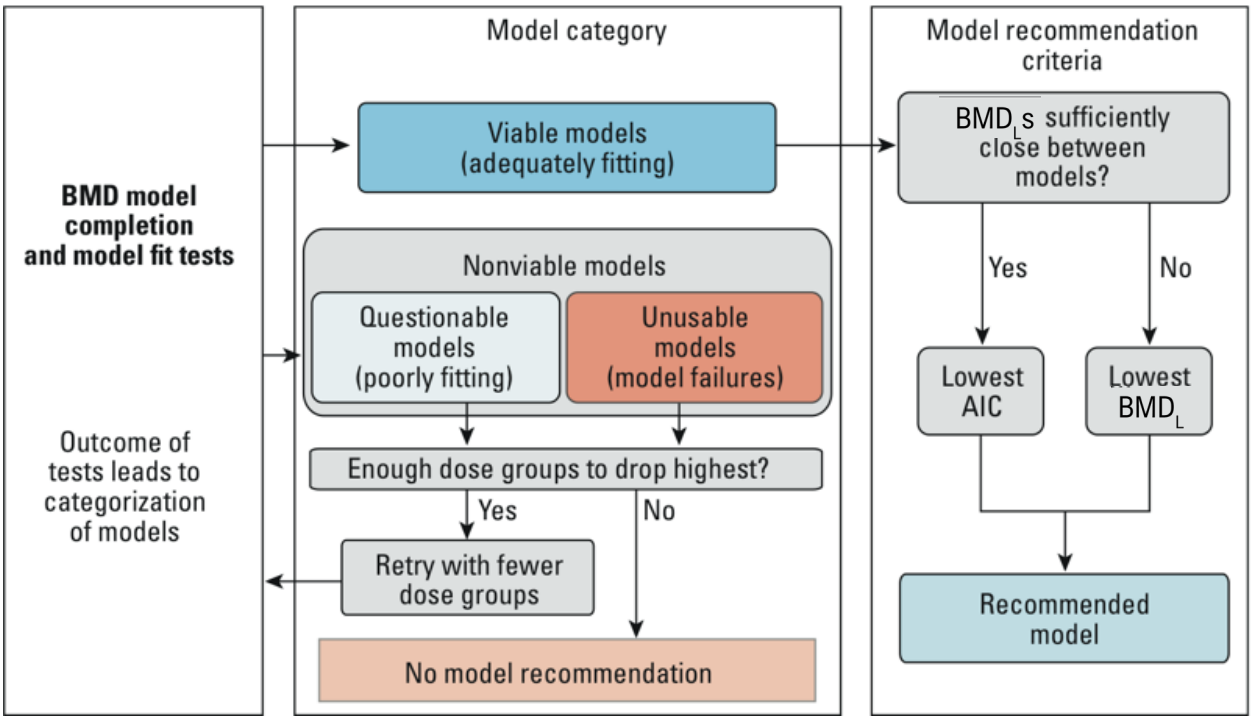

Figure D-1. Benchmark Dose Model Recommendation/Selection Methodology for Automated Benchmark Dose Execution of Apical Endpoints

Source: Figure adapted from Wignall et al. (2014)[23]
BMD = benchmark dose; BMD_L = benchmark dose lower confidence limit; AIC = Akaike information criterion.

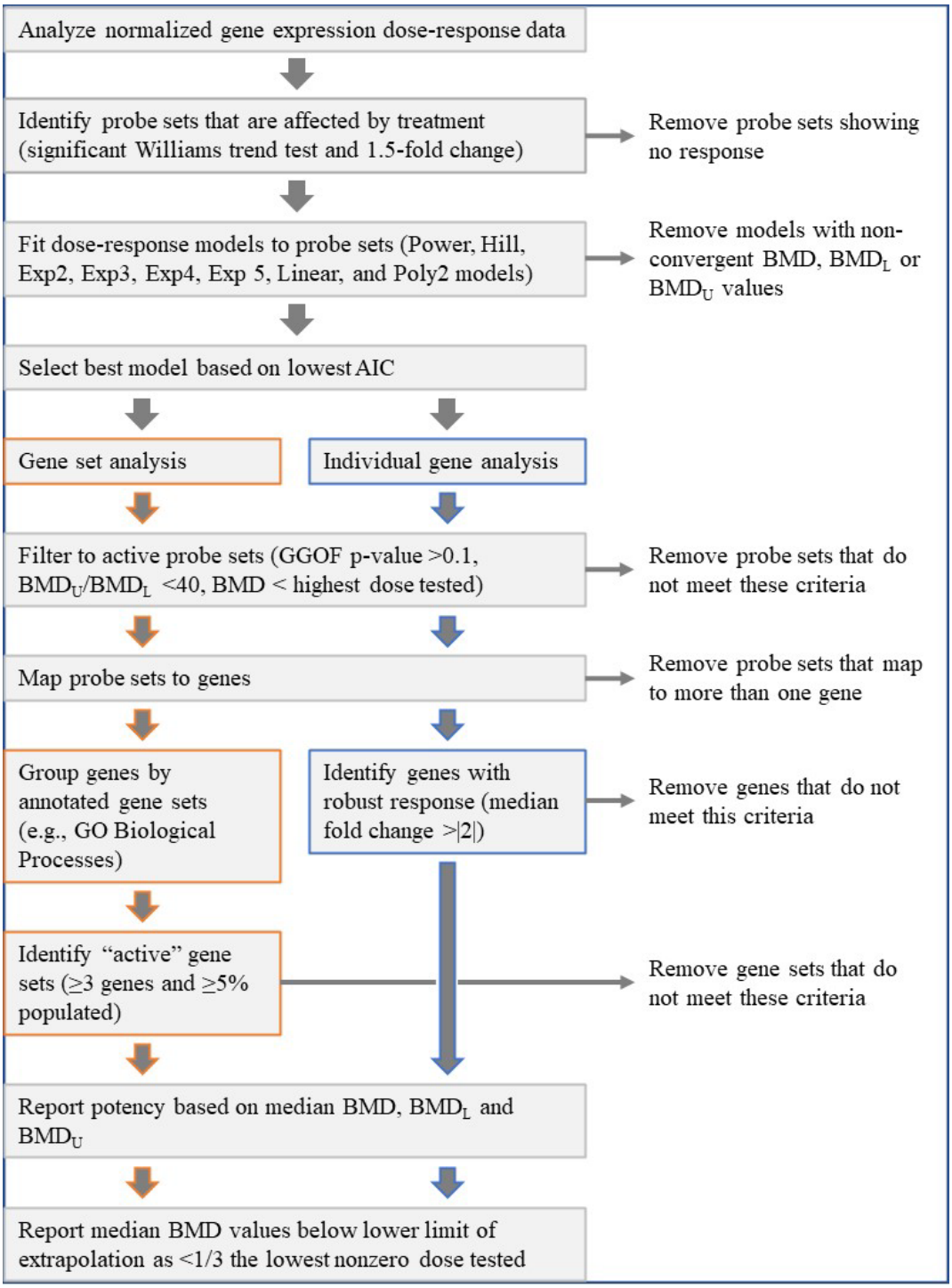

Figure D-2. Benchmark Dose Model Recommendation/Selection Methodology for Benchmark Dose Execution of Gene Sets with Expression Changes Enacted by Chemical Exposure

Adapted from Thomas et al. (2007)[34]
Exp = exponential; Poly = polynomial; BMD = benchmark dose; BMD_L = benchmark dose lower confidence limit; BMD_U = benchmark dose upper confidence limit; AIC = Akaike information criterion; GGOF = global goodness of fit; GO = Gene Ontology.

Appendix E. Organ Weight Descriptions

Table of Contents

E.1. Organ Weight Descriptions

Liver: The liver carries out biotransformation and excretion of endogenous and xenobiotic substances, regulation of blood sugar, enzymatic transformation of essential nutrients, generation of blood proteins involved in fluid balance and clotting, and bile production for digestion and absorption of fats. Liver weight changes can be an indication of chemical-induced stress. Specifically, in subacute studies, increases in liver weight in response to low doses of toxicants typically stem from increases in xenobiotic metabolizing enzymes and associated hepatocyte hypertrophy or peroxisome proliferation. Increased liver weight, particularly when accompanied by evidence of leakage of liver-specific enzymes into blood, likely reflects hemodynamic changes related to severe hepatotoxicity. Higher liver weight relative to body weight may also occur at any dose level that causes a slowed rate of body growth and does not necessarily indicate liver toxicity. Decreased liver weight in subacute studies is typically of unknown toxicological significance but in rare cases may be related to glycogen depletion.

Kidney: The kidneys remove waste products and xenobiotics from the body, balance blood electrolytes, regulate blood pressure through the release of hormones, synthesize the active form of vitamin D, and control the production of erythropoiesis. In subacute studies, changes in kidney weight may reflect renal toxicity (particularly if accompanied by increases in other markers of kidney toxicity, e.g., increased Kim-1) and/or tubular hypertrophy. Decreased kidney weights in subacute studies are typically of unknown toxicological significance.

Heart: The heart drives the circulatory system, supplying oxygen and essential macro- and micronutrients to the tissues. Increased heart weight in subacute studies would indicate severe cardiotoxicity, compensatory myocardial hypertrophy, and/or pulmonary injury. Decreased heart weight in subacute studies is often of unknown toxicological significance; however, it may be caused by decreased load on the heart from dehydration or modulation of contractility.

Appendix F. Supplemental Data

The following supplemental files are available at https://doi.org/10.22427/NIEHS-DATA-NIEHS-10.[29]

F.1. Apical Benchmark Dose Analysis

Mean Body Weight Summary
C20022-01_Mean_Body_Weight_Summary.docx

Organ Weights Summary
C20022-01_Organ_Weights_Summary.docx

Clinical Chemistry Summary
C20022-01_Clinical_Chemistry_Summary.docx

Hematology Summary
C20022-01_Hematology_Data_Summary.docx

Hormone and Enzymes Summary
C20022-01_Hormone_Summary.docx

BMD, NOEL and LOEL Summary for Apical Endpoints
C20022-01_BMD_BMDL_LOEL_and_NOEL_Summary_for_Apical_Endpoints_Sorted_by_BMD_LOEL_from_Low_to_High.docx

Male BMD Apical Endpoints Model Fits
C20022-01_Appendix_Male_07282021.docx

Female BMD Apical Endpoints Model Fits
C20022=01_Appendix_Female_07282021.docx

BMD Model Recommendation Selection Rules
C20022-01_Benchmark_Dose_Model_Recommendation_Selection_Rules_for_Apical_Endpoints.docx

Read Me
C20022-01_ReadME.docx

Male Model Parameters
C20022-01_Parameter_Male_07282021.xlsx

Female Model Parameters
C20022-01_Parameter_Female_07282021.xlsx

BMDs code package
C20022-01_bmds.zip

F.2. Genomic Benchmark Dose Analysis

BMDExpress Project File (bm2 format)
C20022-01_EPA_PFAS_Kidney_Overflow_plate_removed_S1500_Plus_Analysis_Traditional.bm2

Top 10 Genes Ranked by Potency of Perturbation_Kidney
C20022-01_Kidney_Top_10_Genes_Ranked_by_Potency_of_Perturbation_Sorted_by_BMD_Median.docx

Top 10 GO Biological Process Gene Sets_Kidney
C20022-01_Kidney_Top_10_GO_Biological_Process_Gene_Sets_Ranked_by_Potency_of_Perturbation_Sorted_by_BMD_Median.docx

Top 10 Genes Ranked by Potency of Perturbation_Liver
C20022-01_Liver_Top_10_Genes_Ranked_by_Potency_of_Perturbation_Sorted_by_BMD_Median.docx

Top 10 GO Biological Process Gene Sets_Liver
C20022-01-01_Liver_Top_10_GO_Biological_Process_Gene_Sets_Ranked_by_Potency_of_Perturbation_Sorted_by_BMD_Median.docx

BMDExpress Expression Data_Kidney_Female
C20022-01_Kidney_PFHxSAm_Female.txt

BMDExpress Expression Data_Kidney_Male
C20022-01_Kidney_PFHxSAm_Male.txt

BMDExpress Expression Data_Liver_Female
C20022-01_Liver_PFHxSAm_Female.txt

BMDExpress Expression Data_Liver_Male
C20022-01_Liver_PFHxSAm_Male.txt

BMDExpress Individual Gene BMD Results_Kidney_Male
C20022-01_Kidney_PFHxSAm_Male_williams_0.05_NOMTC_foldfilter1.5_BMD_S1500_Plus_Rat_GENE_true_true_pval0.1_ratio40_foldchange2_conf0.5.txt

BMDExpress GO Biological Process Deduplicated BMD Results_Kidney_Male
C20022-01_Kidney_PFHxSAm_Male_williams_0.05_NOMTC_foldfilter1.5_BMD_S1500_Plus_Rat_GO_BP_true_true_pval0.1_ratio40_conf0.5_deduplicate.txt

BMDExpress Individual Gene BMD Results_Kidney_Female
C20022-01_Kidney_PFHxSAm_Female_williams_0.05_NOMTC_foldfilter1.5_BMD_S1500_Plus_Rat_GENE_true_true_pval0.1_ratio40_foldchange2_conf0.5.txt

BMDExpress GO Biological Process Deduplicated BMD Results_Kidney_Female
C20022-01_Kidney_PFHxSAm_Female_williams_0.05_NOMTC_foldfilter1.5_BMD_S1500_Plus_Rat_GO_BP_true_true_pval0.1_ratio40_conf0.5_deduplicate.txt

BMDExpress Individual Gene BMD Results_Liver_Male
C20022-01_Liver_PFHxSAm_Male_williams_0.05_NOMTC_foldfilter1.5_BMD_S1500_Plus_Rat_GENE_true_true_pval0.1_ratio40_foldchange2_conf0.5.txt

BMDExpress GO Biological Process Deduplicated BMD Results_Liver_Male
C20022-01_Liver_PFHxSAm_Male_williams_0.05_NOMTC_foldfilter1.5_BMD_S1500_Plus_Rat_GO_BP_true_true_pval0.1_ratio40_conf0.5_deduplicate.txt

BMDExpress Individual Gene BMD Results_Liver_Female
C20022-01_Liver_PFHxSAm_Female_williams_0.05_NOMTC_foldfilter1.5_BMD_S1500_Plus_Rat_GENE_true_true_pval0.1_ratio40_foldchange2_conf0.5.txt

BMDExpress GO Biological Process Deduplicated BMD Results_Liver_Female
C20022-01_Liver_PFHxSAm_Female_williams_0.05_NOMTC_foldfilter1.5_BMD_S1500_Plus_Rat_GO_BP_true_true_pval0.1_ratio40_conf0.5_deduplicate.txt

BMDExpress Prefilter Results_ Kidney _Female
C20022-01_BMDExpress_Prefilter_Results_Kidney_Female.txt

BMDExpress Prefilter Results_ Kidney _Male
C20022-01_BMDExpress_Prefilter_Results_Kidney_Male.txt

BMDExpress Prefilter Results_ Liver _Female
C20022-01_BMDExpress_Prefilter_Results_Liver_Female.txt

BMDExpress Prefilter Results_ Liver _Male
C20022-01_BMDExpress_Prefilter_Results_Liver_Male.txt

Animal and Fastaq Metadata
C20022-01_Animal_and_FASTQ_Metadata.zip

Kidney Principal Components Analysis Files
C20022-01_Kidney_PCA.zip

Liver Principal Components Analysis Files
C20022-01_Liver_PCA.zip

Individual Gene BMD Analysis Results File
C20022-01_Individual_Gene_Defined_Category_Files_for_Gene_Level_BMD_Analysis_of_Array_Platform_GPL1355.zip

BMDExpress Software
C20022-01_Software.zip

BMDExpress Project File (JSON format)
C20022-01_EPA_PFAS_Kidney_Overflow_plate_removed_S1500_Plus_Analysis_Traditional_JSON.zip

GO Biological Process BMD Analysis Results
C20022-01_Functional_Classification_Annotation_Files_for_GO_Biological_Process_Analysis_of_Array_Platform_GPL1355.zip

F.3. Study Tables

I04 – Mean_Body_Weight_Summary
C20022-01_I04_–_Mean_Body_Weight_Summary.pdf

I05 – Clinical_Observations_Summary
C20022-01_I05_–_Clinical_Observations_Summary.pdf

PA06 – Organ_Weights_Summary
C20022-01_PA06_–_Organ_Weights_Summary.pdf

PA41 – Clinical_Chemistry_Summary
C20022-01_PA41_–_Clinical_Chemistry_Summary.pdf

PA43 – Hematology Summary
C20022-01_PA43_–_Hematology_Summary.pdf

PA48 – Summary of Tissue Concentration
C20022-01_PA48_-_Summary_of_Tissue_Concentration.pdf

R07 – Hormone_Summary
C20022-01_R07_–_Hormone_Summary.pdf

F.4. Individual Animal Data

Individual Animal Body Weight Data
C20022-01_Individual_Animal_Body_Weight_Data.xlsx

Individual Animal Clinical Chemistry Data
C20022-01_Individual_Animal_Clinical_Chemistry_Data.xlsx

Individual Animal Clinical Observations Data
C20022-01_Individual_Animal_Clinical_Observations_Data.xlsx

Individual Animal Hormone Data
C20022-01_Individual_Animal_Hormone_Data.xlsx

Individual Animal Organ Weight Data
C20022-01_Individual_Animal_Organ_Weight_Data.xlsx

Individual Animal Hematology Data
C20022-01_Individual_Animal_Hematology_Data.xlsx

Individual Animal Tissue Concentration Data
C20022-01_Individual_Animal_Tissue_Concentration_Data.xlsx

National Institute of
Environmental Health Sciences
Division of Translational Toxicology
Office of Policy, Review, and Outreach
P.O. Box 12233
Durham, NC 27709

www.niehs.nih.gov/reports

ISSN 2768-5632